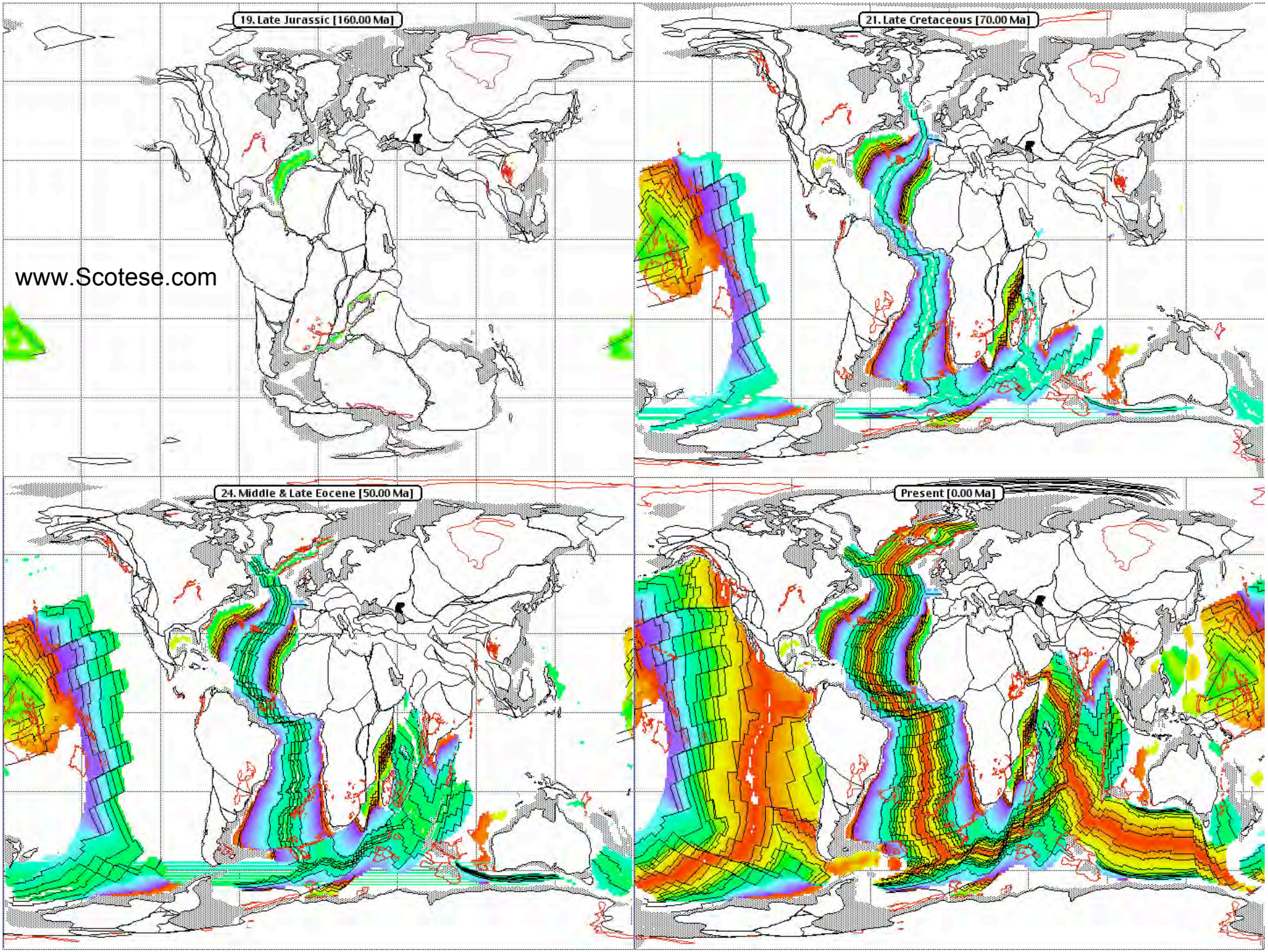
19. Late Jurassic [160.00 Ma]
21. Late Cretaceous [70.00 Ma]
www.Scotese.com
24. Middle & Late Eocene [50.00 Ma]
Present [0.00 Ma]

Tucholke and Fry 1985

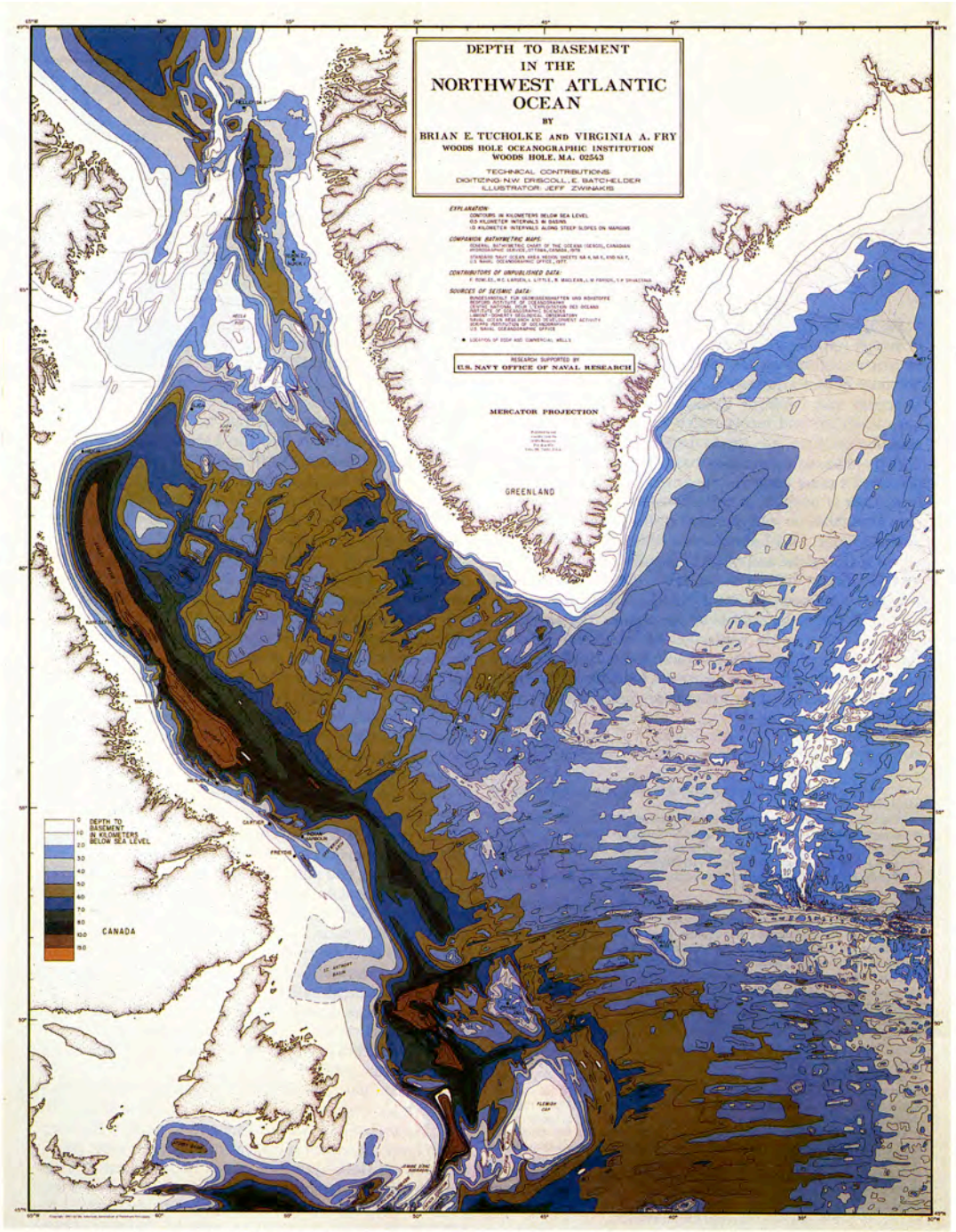

Figure 1—Depth to basement, in kilometers below sea level, in northwest Atlantic Ocean. Locations of DSDP and commercial wells summarized in Figure 5 are shown. Track control is indicated by fine dotted lines. St. Anthony and Sydney basins and two small basins near Newfoundland are principally Paleozoic features (Wade et al., 1977); they are enclosed by dashed contours.

Tucholke and Fry 1985

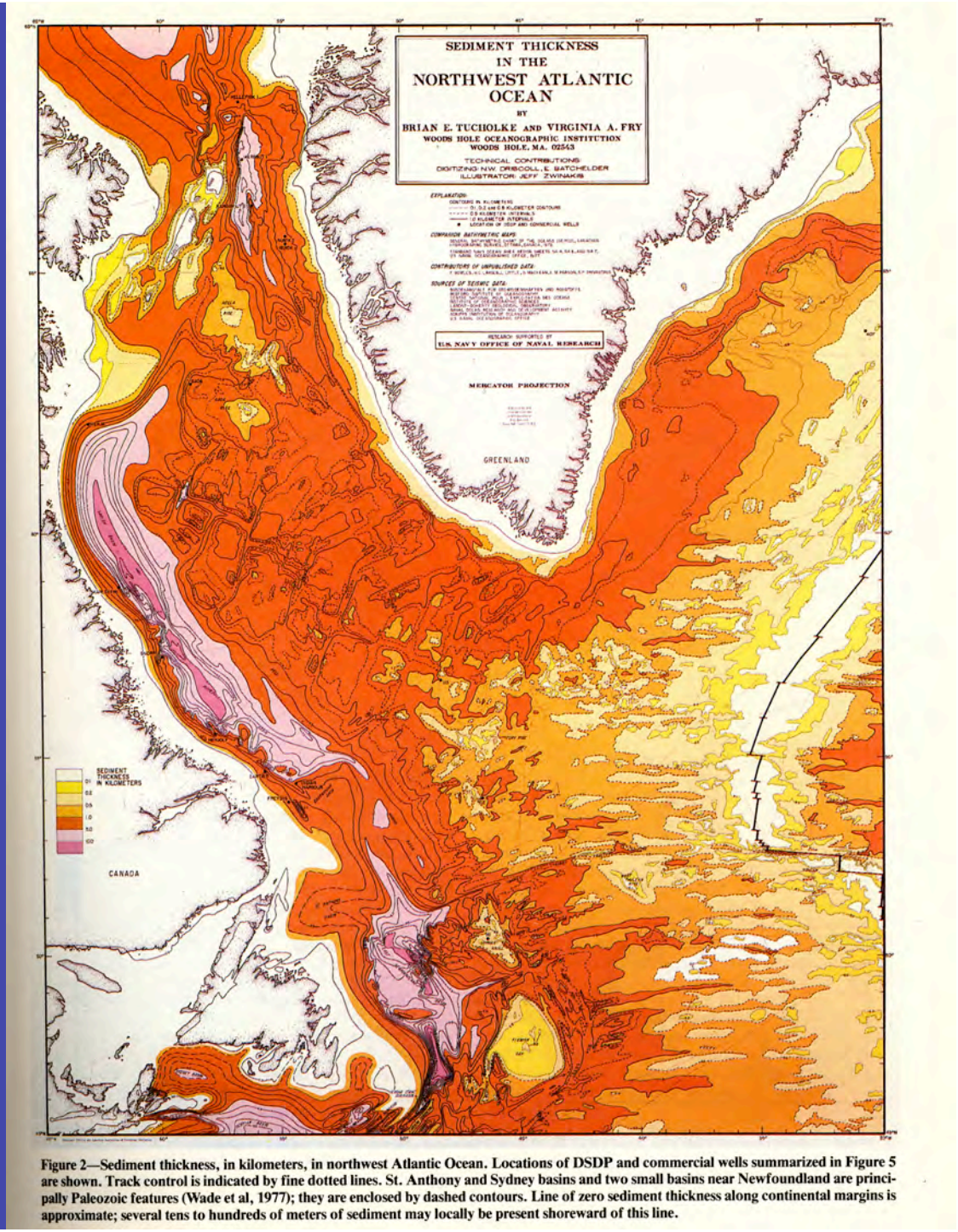

Figure 2—Sediment thickness, in kilometers, in northwest Atlantic Ocean. Locations of DSDP and commercial wells summarized in Figure 5 are shown. Track control is indicated by fine dotted lines. St. Anthony and Sydney basins and two small basins near Newfoundland are principally Paleozoic features (Wade et al, 1977); they are enclosed by dashed contours. Line of zero sediment thickness along continental margins is approximate; several tens to hundreds of meters of sediment may locally be present shoreward of this line.

Marine Geology of Sohm Basin, Canadian Margin

Ebinger and Tucholke 1988

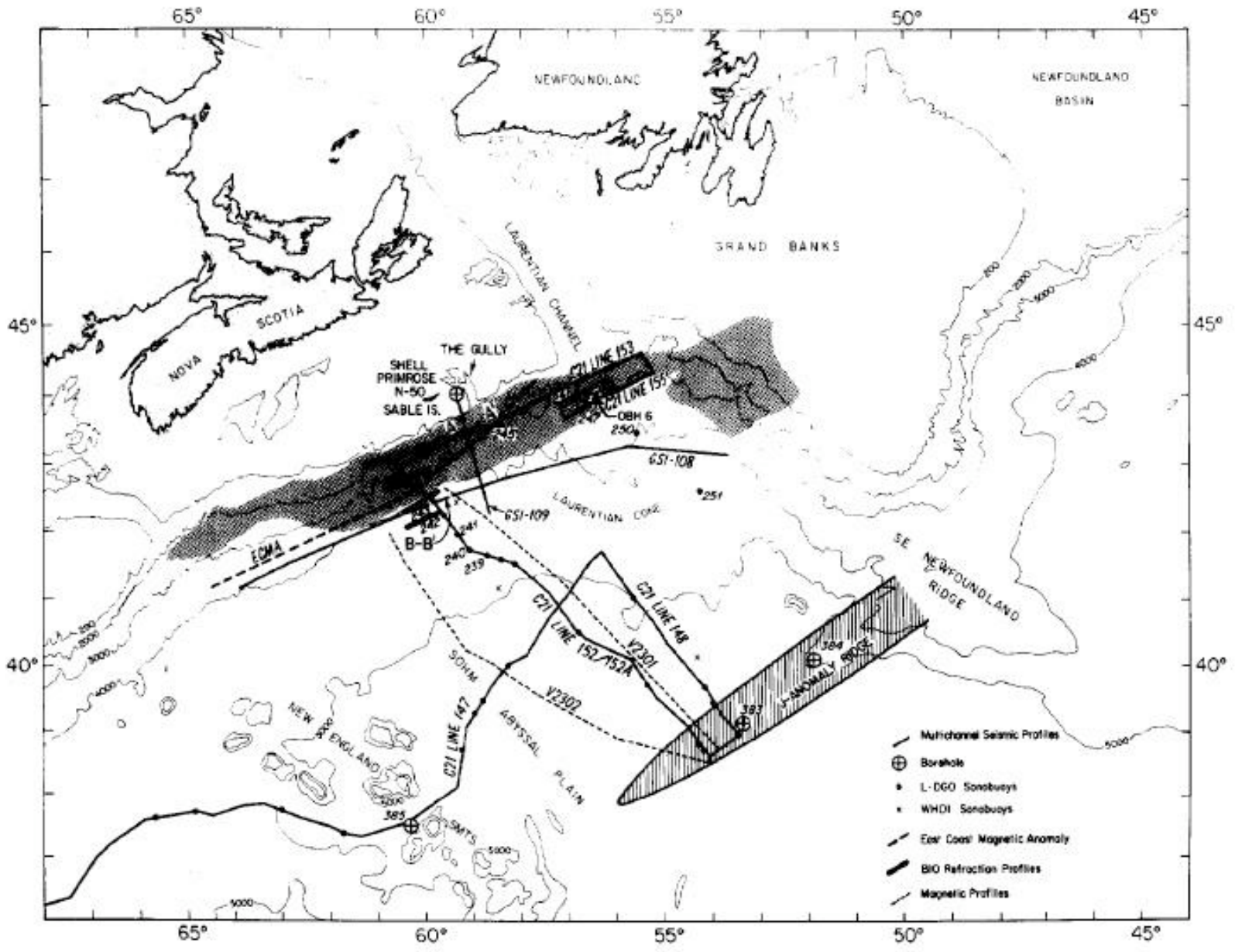

Figure 1—Bathymetric location map (depths in corrected meters) of Sohm basin, showing basin boundaries formed by New England Seamount Chain, J-Anomaly Ridge, and continental margin of Nova Scotia and Grand Banks. Approximate distribution of salt-ridge province is indicated by stippled pattern. Segments of MCS profiles illustrated in Figures 11 and 12 indicated by AA′ and BB′, respectively. Scale: 1½ cm = 220 km.

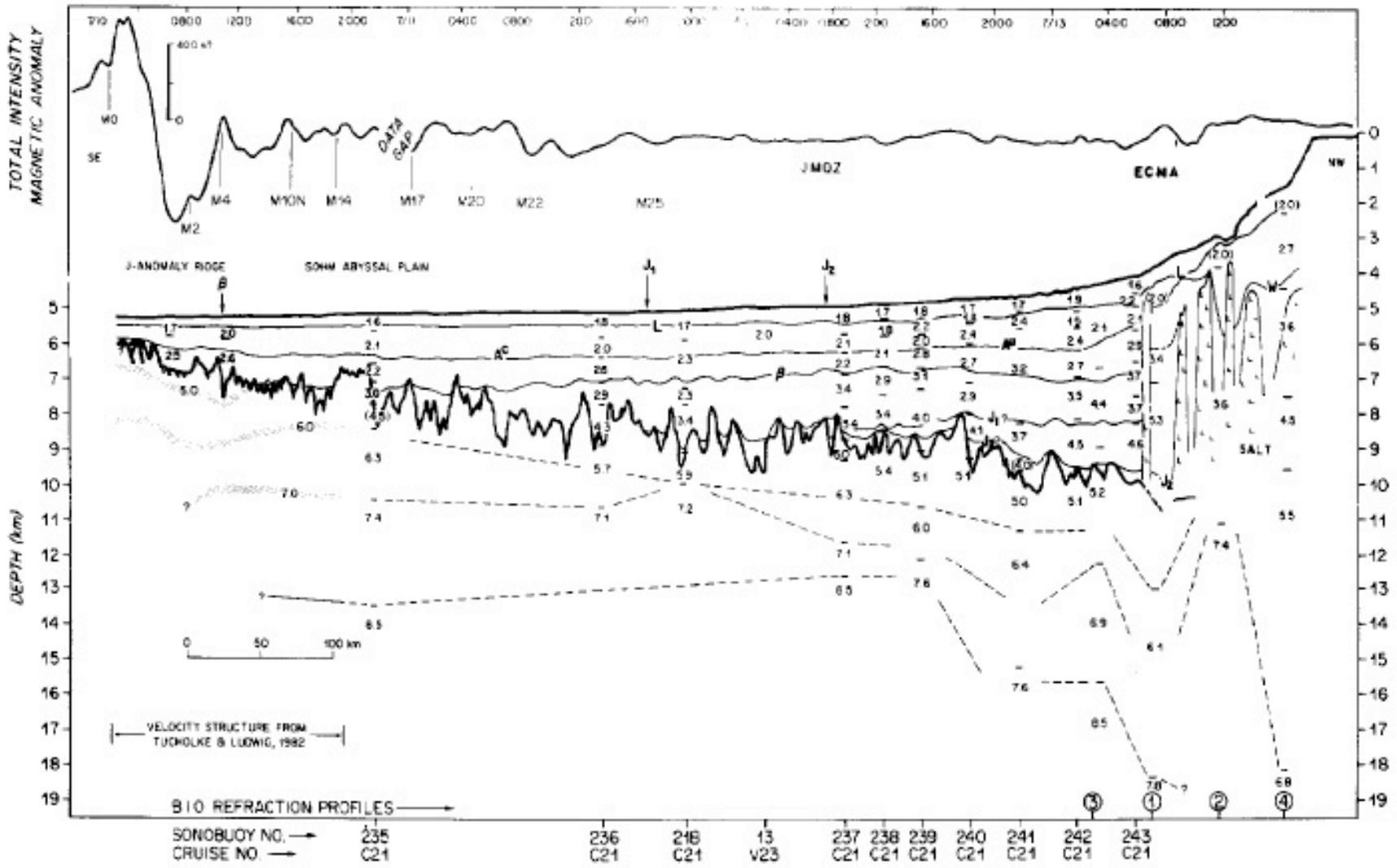

Figure 3—Depth section across Sohm Abyssal Plain and Nova Scotian continental rise along line of reflection profile C21 152/152A; location in Figure 1. Westward extension of section onto continental shelf is schematic. Sonobuoy layer solutions are as in Table 1; sonobuoy identifications are given across bottom of figure. Refraction velocities beneath J-Anomaly Ridge are shown as isovelocity contours (stippled pattern) (from Tucholke and Ludwig, 1982); velocities beneath continental rise are from Keen et al (1975). Vertical exaggeration is 22.5:1. Pinch-outs of reflections J_2, J_1, and β are designated by arrows. Magnetic anomaly profile is shown detrended, with anomaly identifications based on models discussed in text.

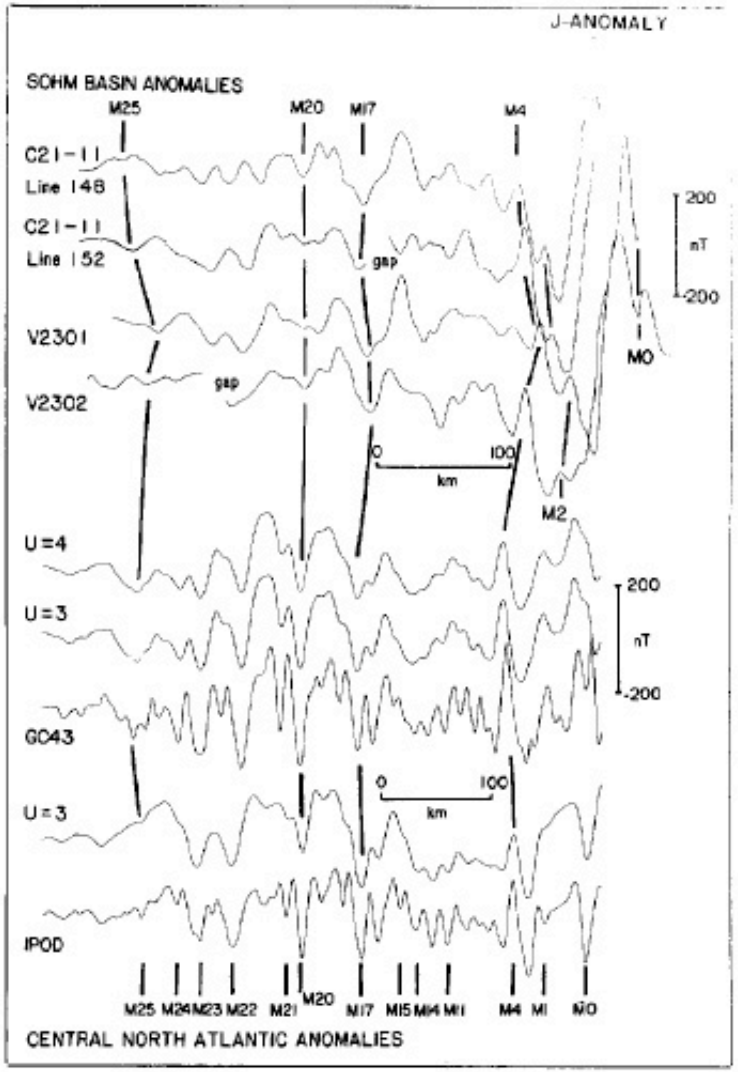

Figure 4—Top: observed Mesozoic magnetic anomalies (zero meaned, detrended) along *Conrad* 21 lines 148 and 152 and along *Vema* 2301 and 2302 cruise tracks across Sohm basin; locations in Figure 1. Bottom: Mesozoic magnetic anomalies along *Glomar Challenger* Leg 43 and IPOD-USGS tracks in central North Atlantic south of Bermuda. Filtered versions of profiles were phase shifted by 30° and continued upward (U, in kilometers) to replicate slower spreading rates and greater depth to magnetic source layer in Sohm basin.

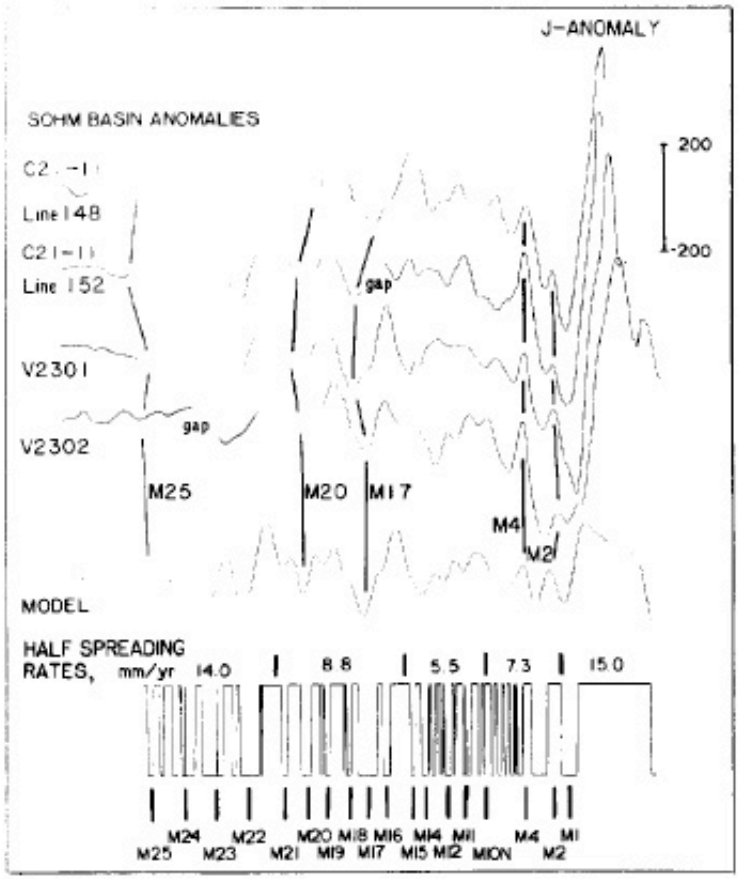

Figure 5—Top: Mesozoic magnetic anomalies across Sohm basin as in Figure 4. Bottom: forward model constructed from Mesozoic reversal sequence of Larson and Hilde (1975) and filtered to simulate observed depths to basement and slow spreading rates as described in text. Magnetic layer thickness is 2 km and magnetization is 10 emu/cm^3. No attempt was made to model high-amplitude J-Anomaly. Spreading rates are based on geomagnetic polarity time scale of Kent and Gradstein (1986).

1980), and layer 2A (<4.1 km/sec) is either absent or too thin to be detected. The generally observed increase in upper crustal velocities with crustal age (i.e., the disappearance of layer 2A) is thought to be caused by crustal

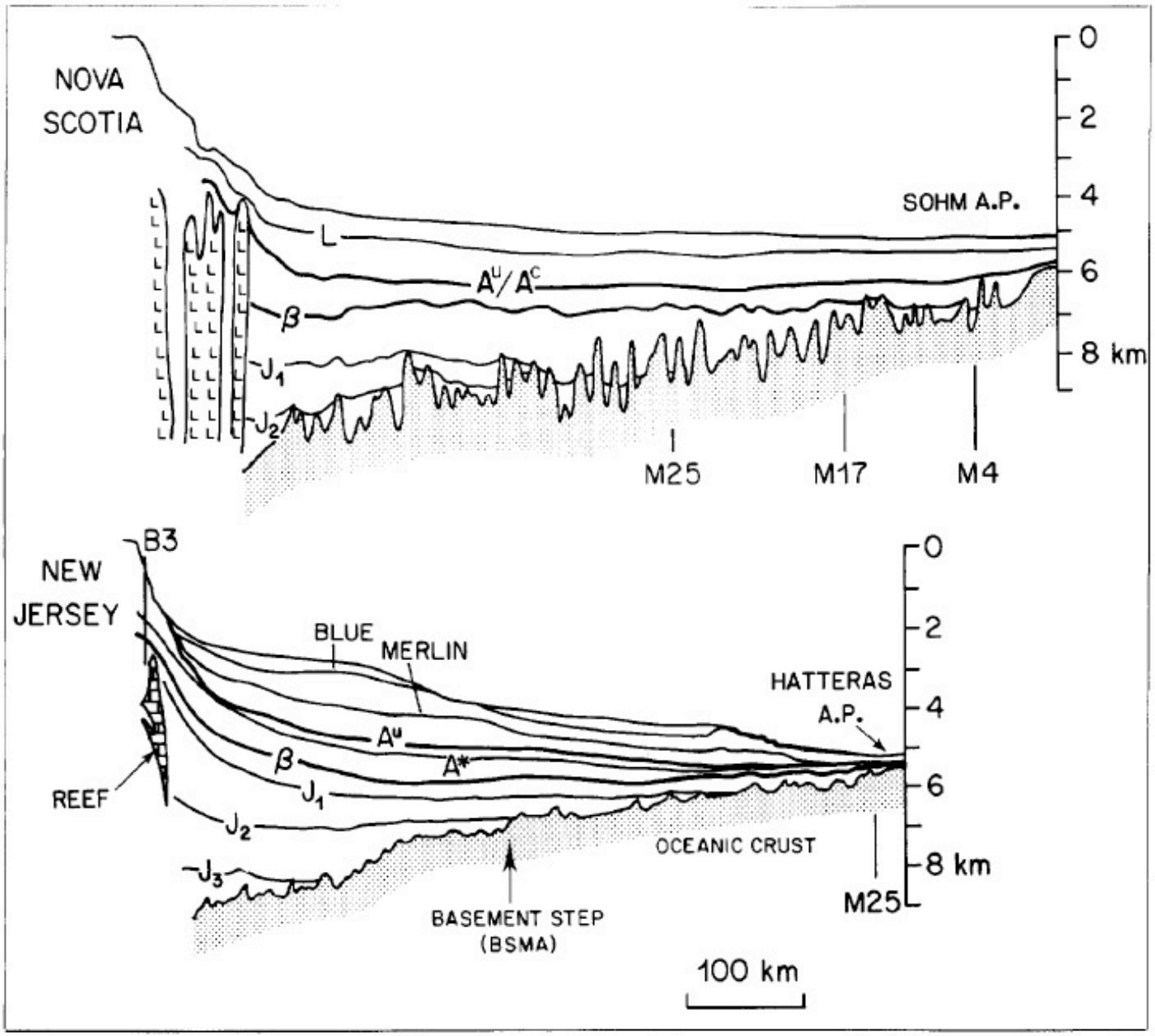

Figure 6—Simplified stratigraphic cross sections of Nova Scotian continental margin (top) and continental margin off New Jersey (bottom) (from Mountain and Tucholke, 1985). Comparison of Horizons β and A" in two profiles beneath upper continental rise emphasizes differences in subsidence behavior of lithosphere along two margins. Thermal subsidence along Nova Scotian margin is greater, probably having continued into Tertiary.

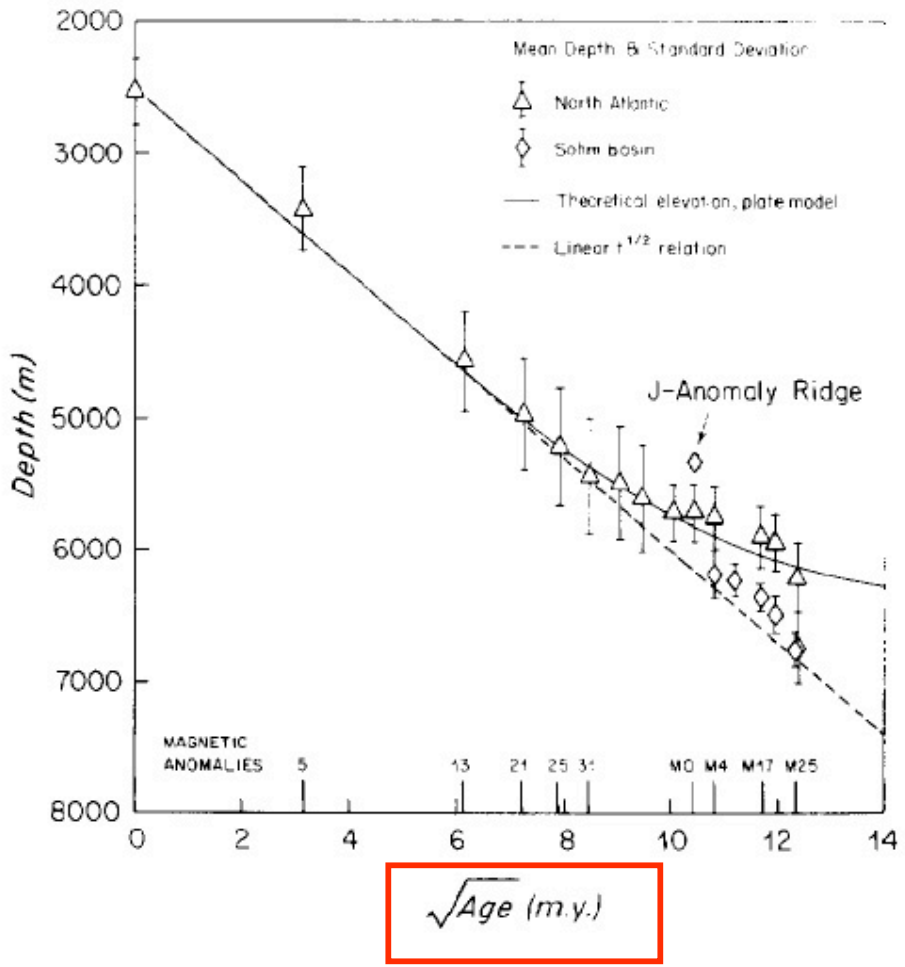

Figure 7—Mean values and standard deviations of basement depth (corrected for sediment loading) plotted vs. square root of age, $t^{1/2}$, for Sohm basin (diamonds), compared to entire North Atlantic (triangles) as determined by Parsons and Sclater (1977). Predicted values for a linear $t^{1/2}$ dependence and for a cooling-plate model (Parsons and Sclater, 1977) are shown as dashed and solid lines, respectively. Basement depth of J-Anomaly Ridge at anomaly M0 has not been corrected to account for its probable subaerial formation (Tucholke and Ludwig, 1982).

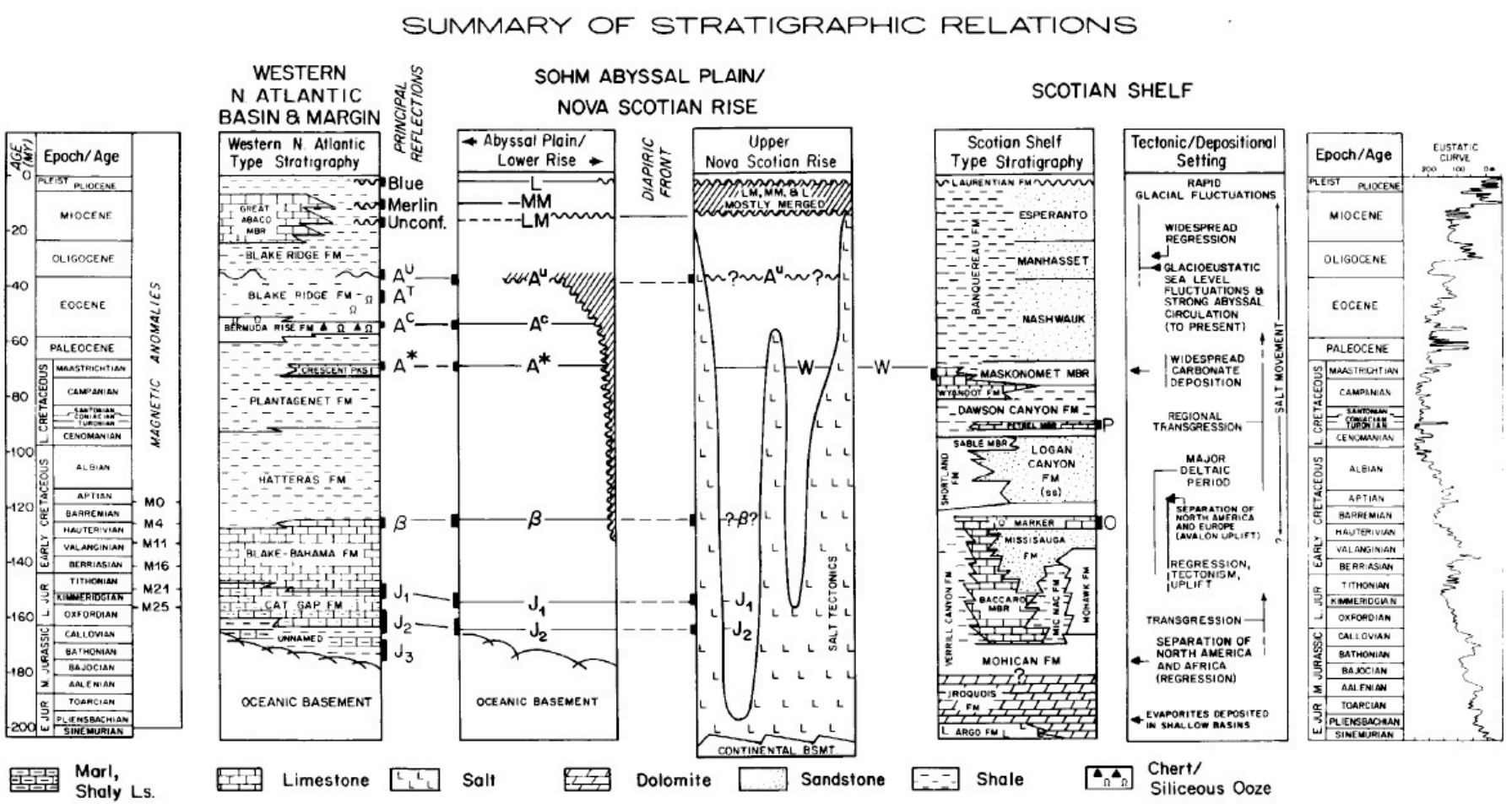

Figure 8—Summary of rock- and seismic-stratigraphic relations in western North Atlantic. From left, basin and margin south of New England Seamount Chain, Sohm basin as presented in this paper, Nova Scotian continental shelf, and global sea level fluctuations. Bold bars adjacent to columns 2, 3, 4, and 5 indicate age range of seismic horizons described in text. Correlations between columns tentative where dashed. Data sources: timescale, Kent and Gradstein (1986); western North Atlantic lithology, Jansa et al (1979); seismic horizons, Tucholke and Mountain (1979), Klitgord and Grow (1980); Sohm basin and rise seismic horizons, Uchupi and Austin (1979b), King (1975), Stow (1981), Suitt et al (1986), and this paper; Scotian shelf lithology, McIver (1972), Jansa and Wade (1975), Given (1977); Scotian margin tectonic setting, Jansa and Wade (1975), Barrett and Keen (1976); global sea level curve, Haq et al (1987).

Sohm Basin, Canadian Atlantic Margin

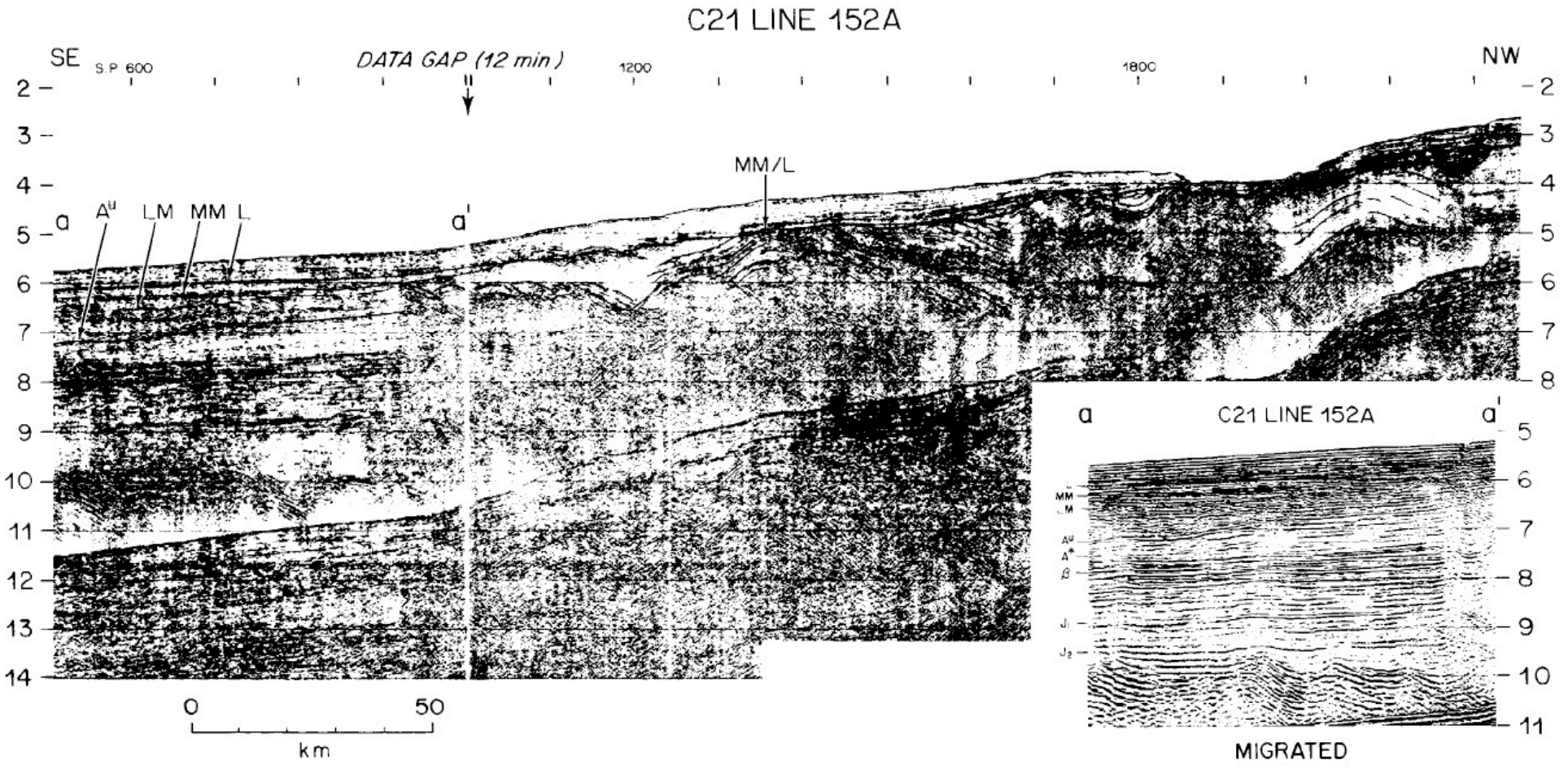
C21 LINE 152A
SE
S.P. 600
DATA GAP (12 min.)
1200
1800
NW
a
A^u
LM
MM
L
a'
MM/L
0
50
km
a
C21 LINE 152A
a'
MM
LM
A^u
A*
B
J1
J2
MIGRATED

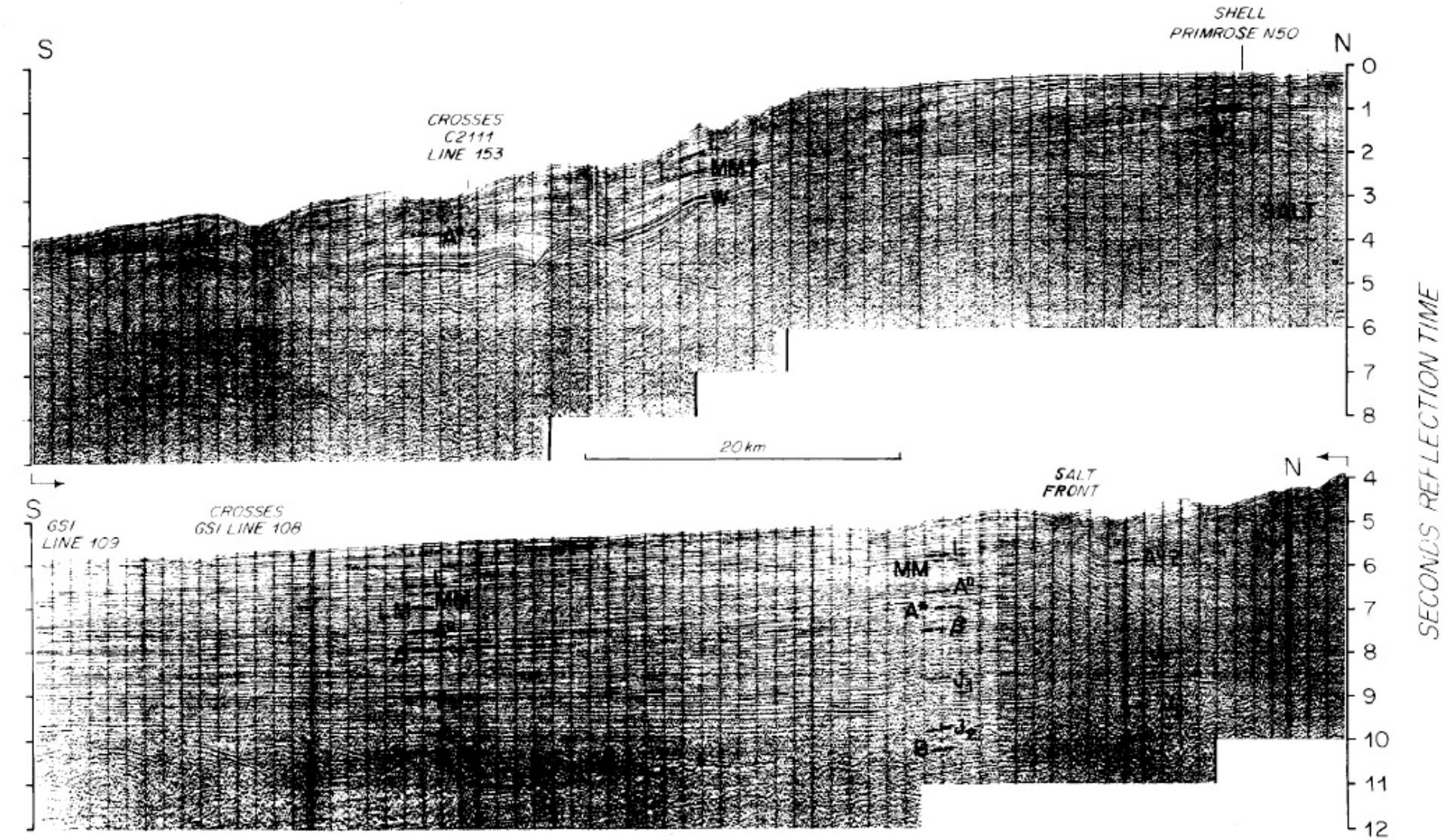

Figure 10—Segment of GSI MCS line 109 across Nova Scotian continental shelf and rise; location in Figure 1. Note well-developed reflection from Wyandot chalk (W), which was penetrated in Shell N-50 Primrose well. Also note Pliocene-Pleistocene foreset beds developed above Horizon L on outer continental shelf. See Figure 8 for correlation of reflections to age and lithology.

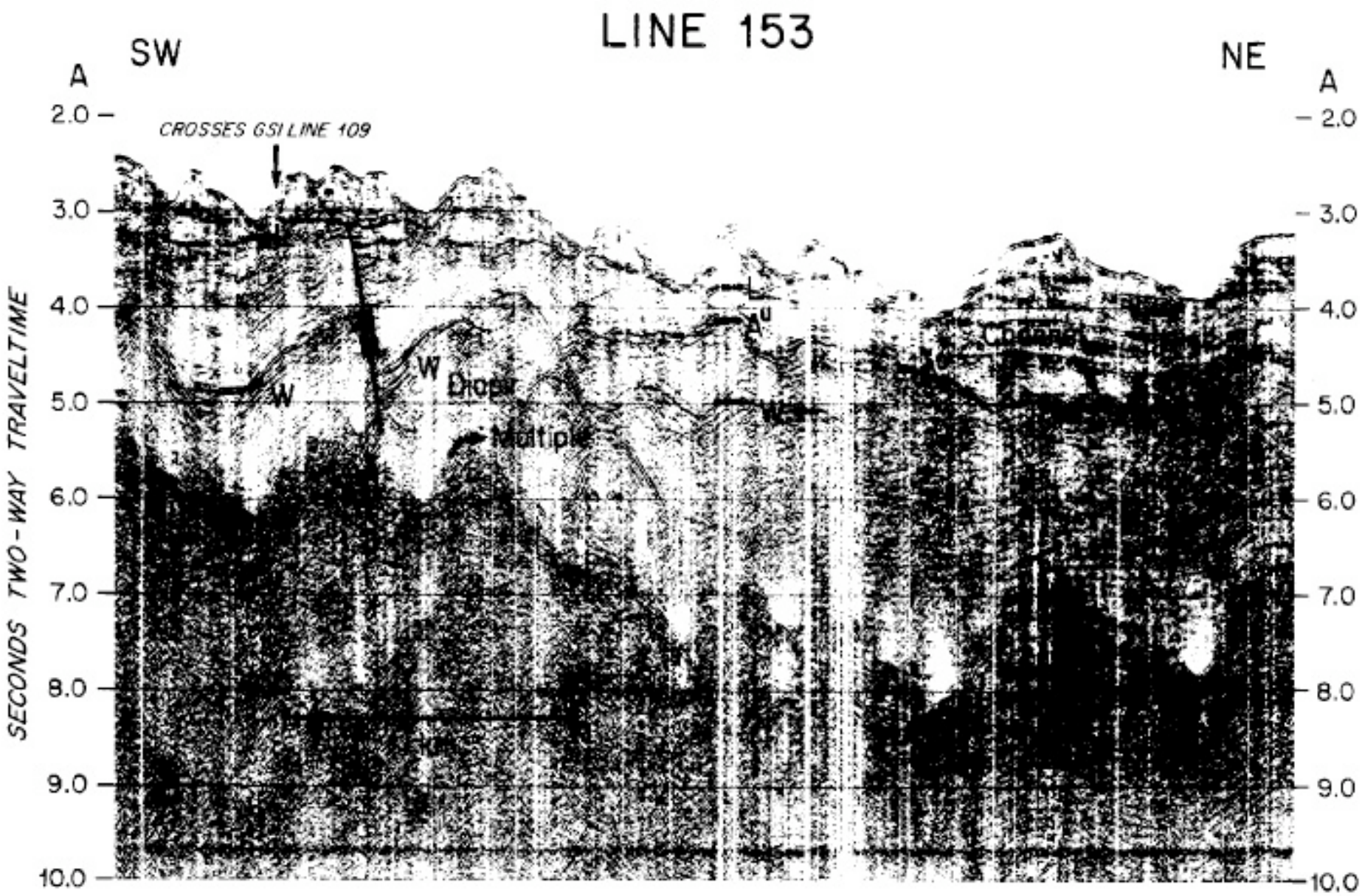

Figure 11—Segment of *Conrad* 21 line 153 along strike of central Nova Scotian continental rise; location in Figure 1. Note channel defined by Horizon A" at right; this probably represents re-excavation of original A" unconformity by cross-slope erosion during middle Oligocene sea level lowstand (see text). Lack of deformation of Horizon L suggests little salt movement has occurred on this part of continental rise since late Pliocene; seismic sequences above Horizon L clearly show erosion and syndepositional formation of canyons and channels during Quaternary.

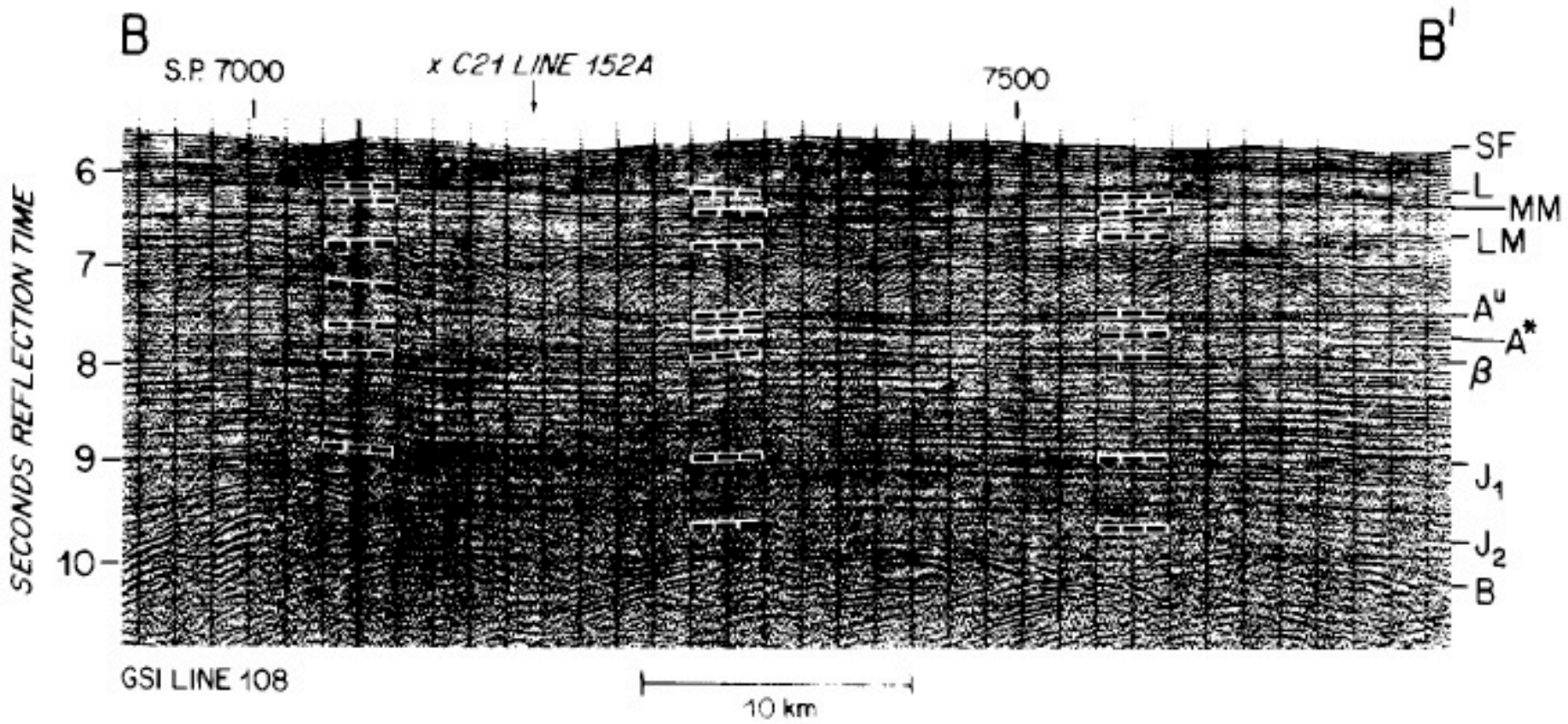

Figure 12—Segment of GSI MCS line 108 along strike of Nova Scotian lower continental rise; location in Figure 1. Note truncation of underlying reflections at Horizon A^u (left) and abrupt change in seismic character from flat reflections below Horizon A^u to diffracting horizons above. See Figure 8 for correlation of reflections to age and lithology.

Conclusions

- Ocean crust beneath Sohm basin generated slowly: 5-15 mm/year
- Ocean floor topography is very rough
- Ocean crust is “normal”, ~ 5 km
- Ocean crust subsidence is less than normal, suggesting cold, dense aesthnosphere
- New England Seamounts did not effect seds
- Salt diapirs on continental rise effect seds
- Glacio-eustatic variations related to thick Quaternary sediments

Basin Evolution in Southern East Greenland: An Outcrop for Cretaceous-Paleogene Basin on the North Atlantic Volcanic Margins

Larsen, Hamberg, Olaussen,
Norgaard-Pedersen and Stemmerik

1999

Late Cretaceous Reconstruction Of the North Atlantic showing Postions of UK, Norway, and Greenland

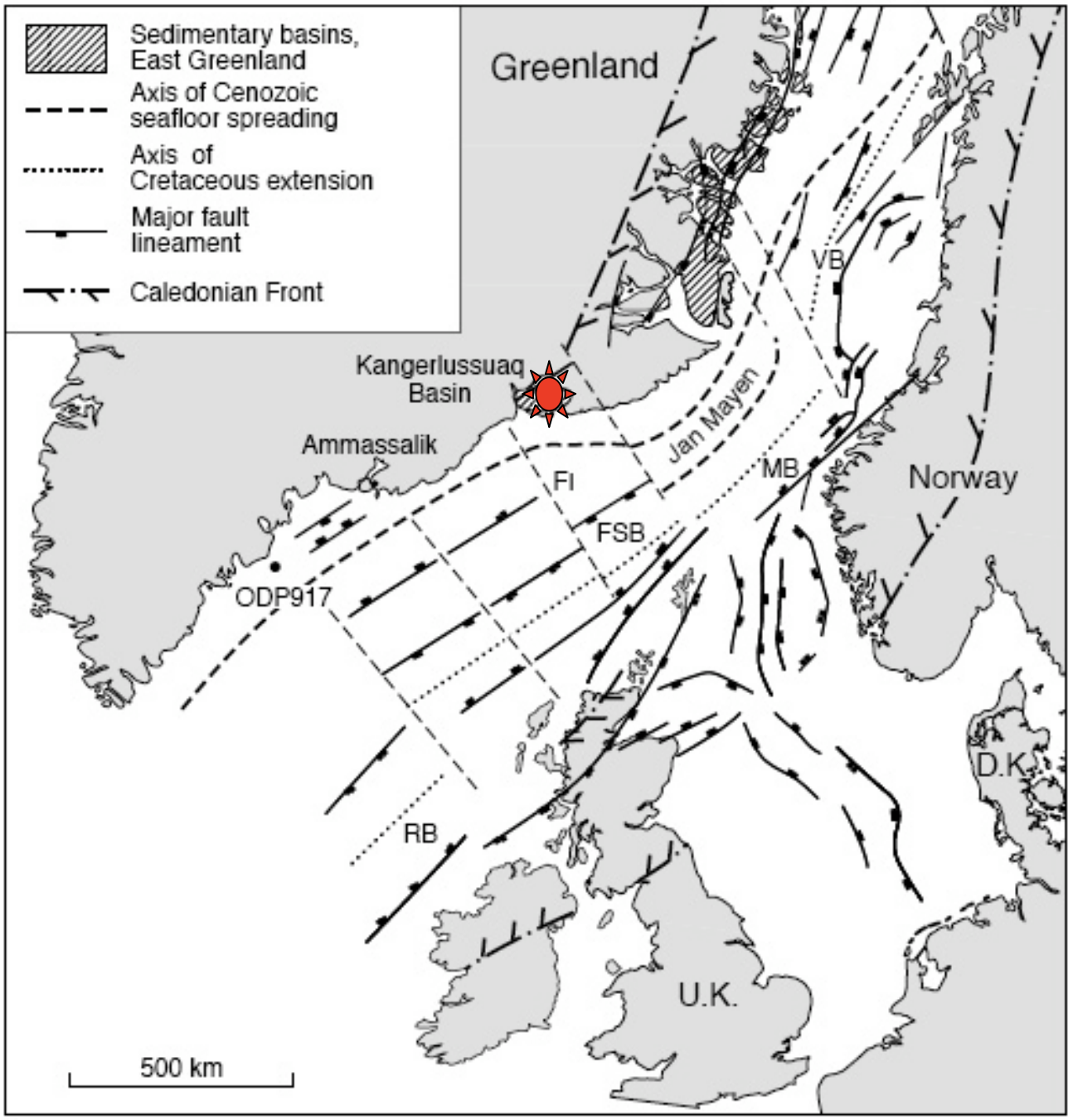


Paleogene plutonic rocks
Paleogene basaltic rocks
U. Paleozoic–Jurassic sediments
Cretaceous–Paleogene sediments
Crystalline basement
Fault
Measured sections
Section referred to in text
Tertiary intrusive centers
Greenland
Traill Ø
Jameson Land
Scoresby Sund
Kap Brewster
Inland Ice
Rømer Fjord
Kap Dalton
Blosseville Kyst
Kangerlussuaq
Kulhøje
10
Skærmen
Korridoren
CHRISTIAN IV GLETSCHER
Sortekap
7
Pyramiden
SORGENFRI GLETSCHER
KANGERLUSSUAQ
Watkins Fjord
Amdrup Fjord
Sødalen
C. Jacobsen Fjord
Ryberg Fjord
J.A.D. Jensen Fjord
Nansen Fjord
Amdrup Pynt
Miki Fjord
20 km

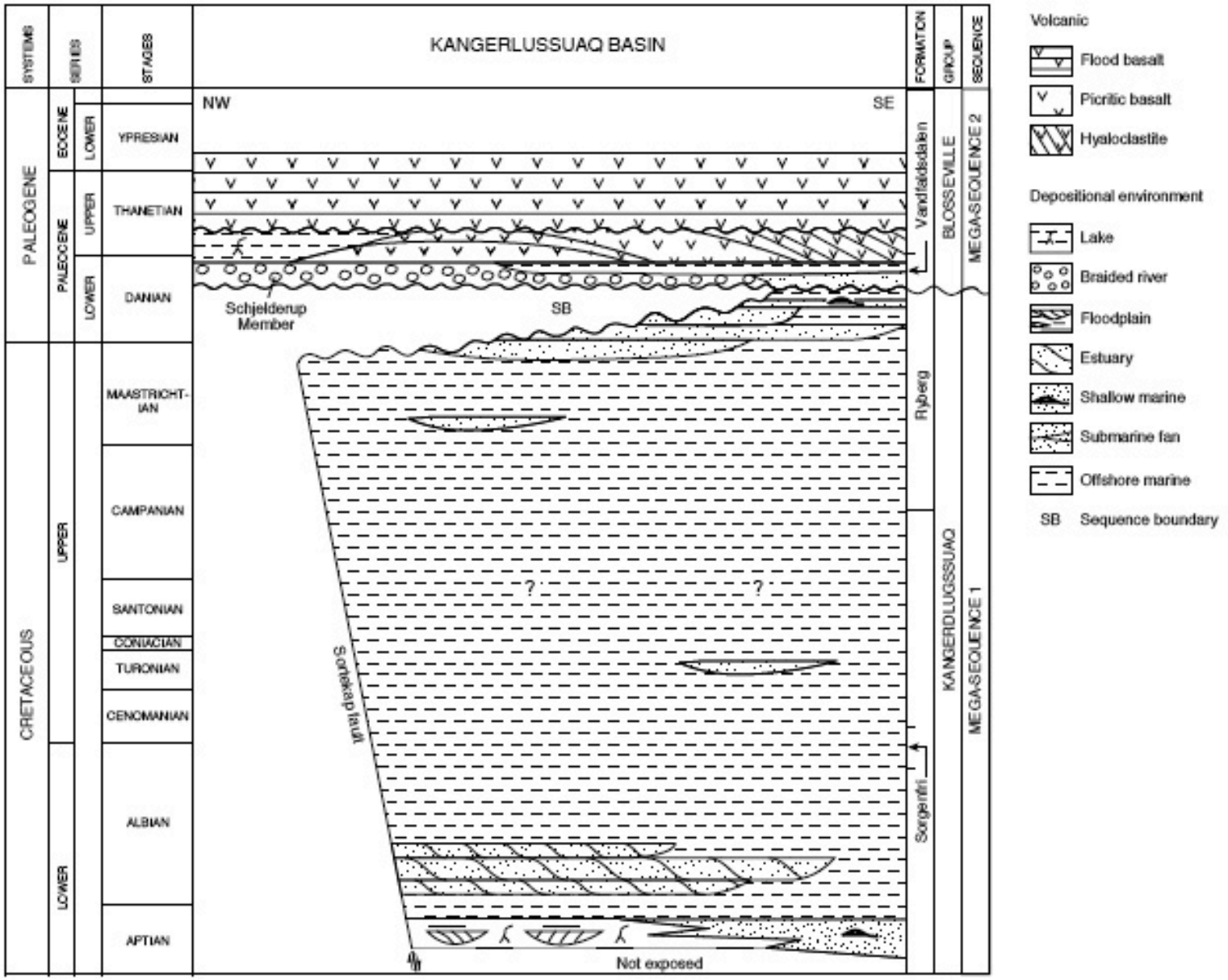

Figure 3—Figure showing the chronostratigraphy and lithostratigraphy of the sedimentary and volcanic succession of the Kangerlussuaq basin. The stratigraphic data are summarized from a number of sections in a generalized northwest–southeast cross section through the basin. Lithostratigraphy is based on Soper et al. (1976a). Time scale from Haq et al. (1988).

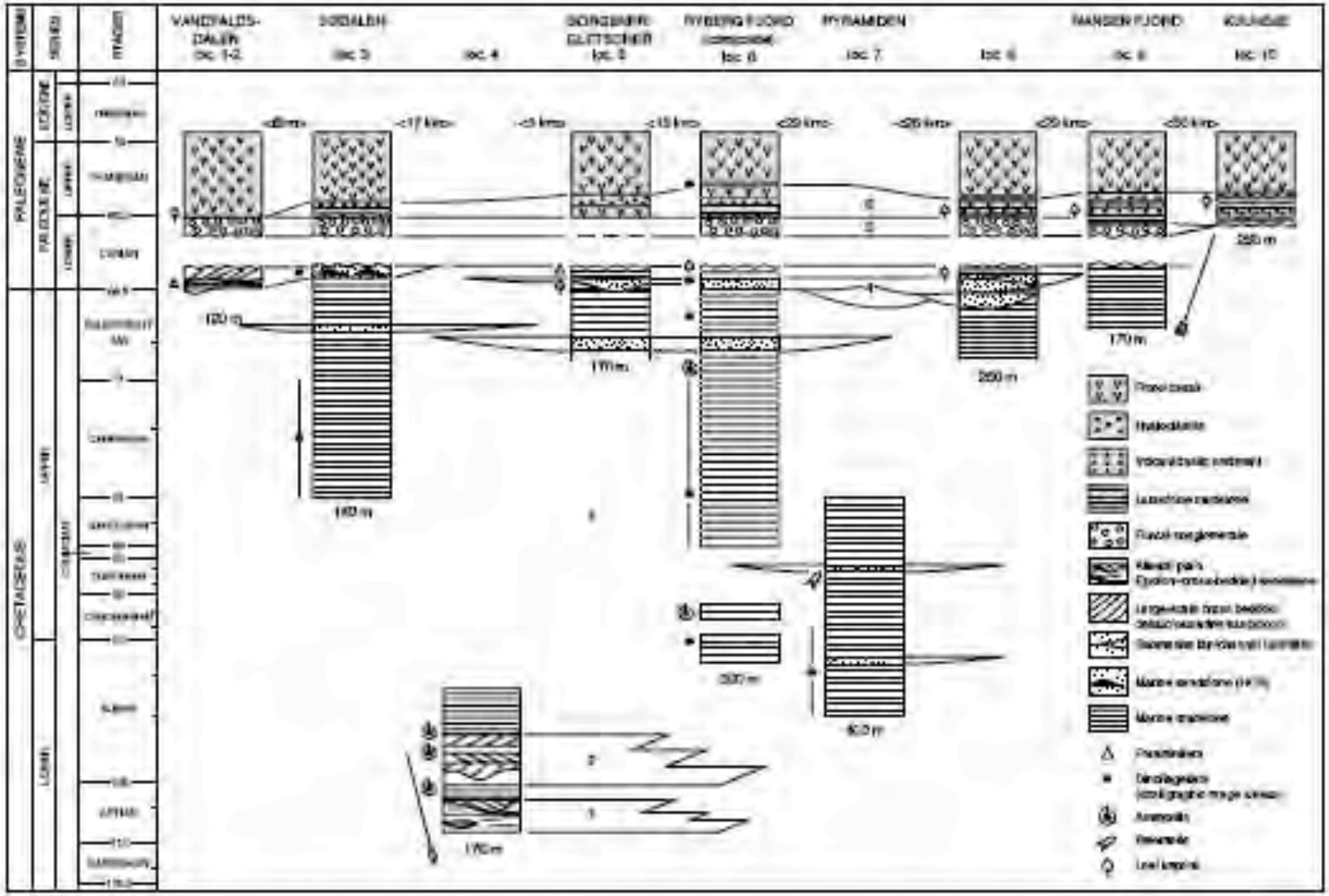

Figure 4—Schematic cross section (see Figure 2 for location) of the Kangerlussuaq basin showing chronostratigraphy and biostratigraphy of selected sections. Major facies associations indicated by numbers: (1) alluvial plain and shallow marine, (2) fluvio-estuarine, (3) offshore marine, (4) submarine fan and channel-levee, (5) fluvial, (6) volcanic. Thickness refers to the measured sedimentary sections and does not include the overlying flood basalts. loc. = location; see Figure 2 for placement of locations. Biostratigraphic data from Soper et al. (1976 a, b), Christensen and Hoch (1983), Hoch (1990), and our own observations. Time scale from Haq et al. (1988).

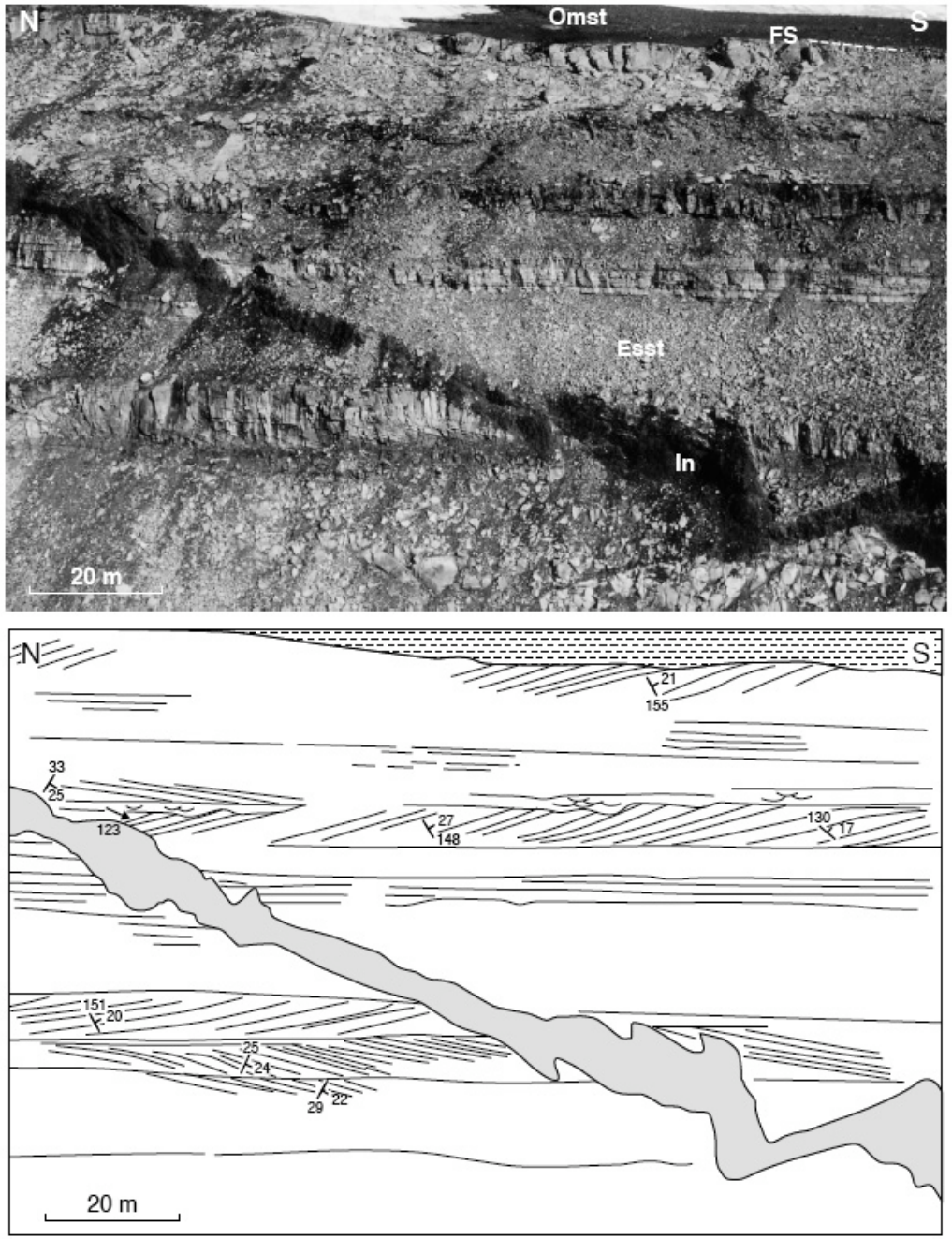

Figure 7—Lower Albian coarse-grained estuarine sandstones (Figure 2, location 4). Note large-scale cross-bedded units up to 15 m thick. Migration was toward the east, into the photograph (see summary of paleocurrent data in Figure 6). Esst = Estuarine sandstones, Omst = Offshore marine mudstones, In = intrusive Paleogene dyke, FS = flooding surface. Height of cliff face approximately 100 m.

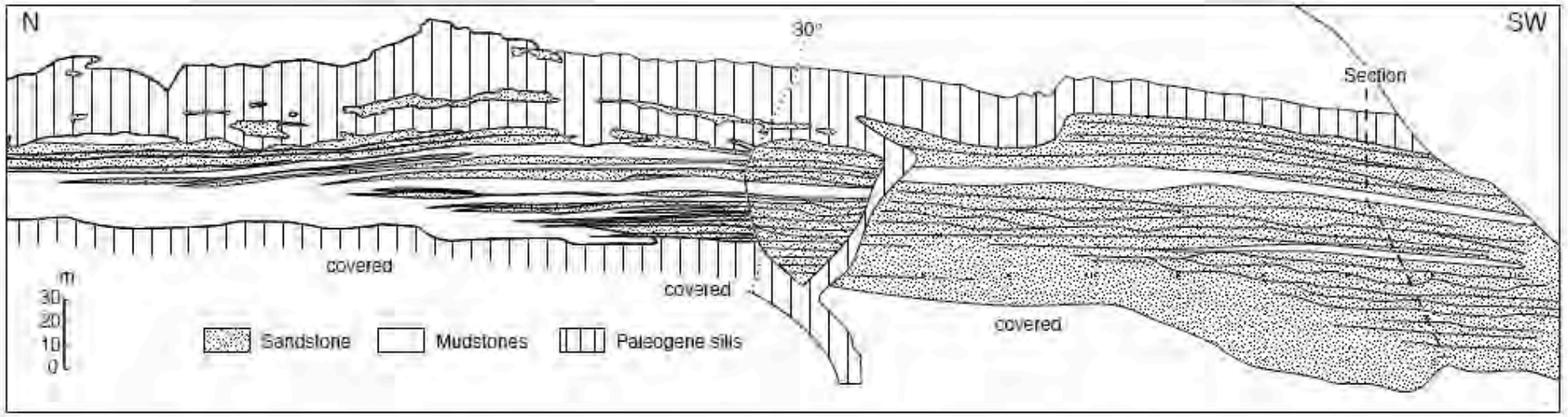

Figure 9—Sketch drawn from a photographic mosaic of a lower Paleocene(?) channel–levee complex exposed east of Sorgenfri Gletcher (Figure 2, location 8 and vertical section shown in Figure 8). Note the wedging out of turbidite sandstones into mudstone-dominated levee deposits toward the northeast (to the left). The succession is strongly intruded by Paleogene basaltic sill complexes.

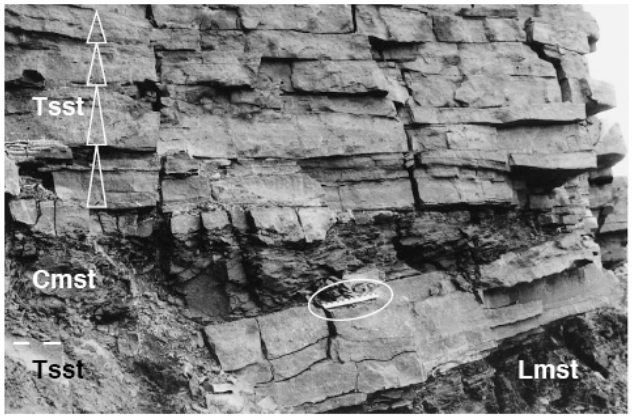

Figure 10—Outcrop photograph of amalgamated medium-grained turbiditic sandstones (Tsst) and contorted, slumped mudstones (Cmst) of the lower Paleocene turbidite succession (Figure 2, location 8). The turbiditic sandstones are graded showing T_{a-c} Bouma divisions. The slumped mudstones are strongly lenticular and occur as subordinate beds in an otherwise sandstone-dominated turbidite succession. They are interpreted as failure of channel margins in periods between active turbidite deposition. Lmst = laminated marine mudstones. Scale (circled) is 20 cm long.

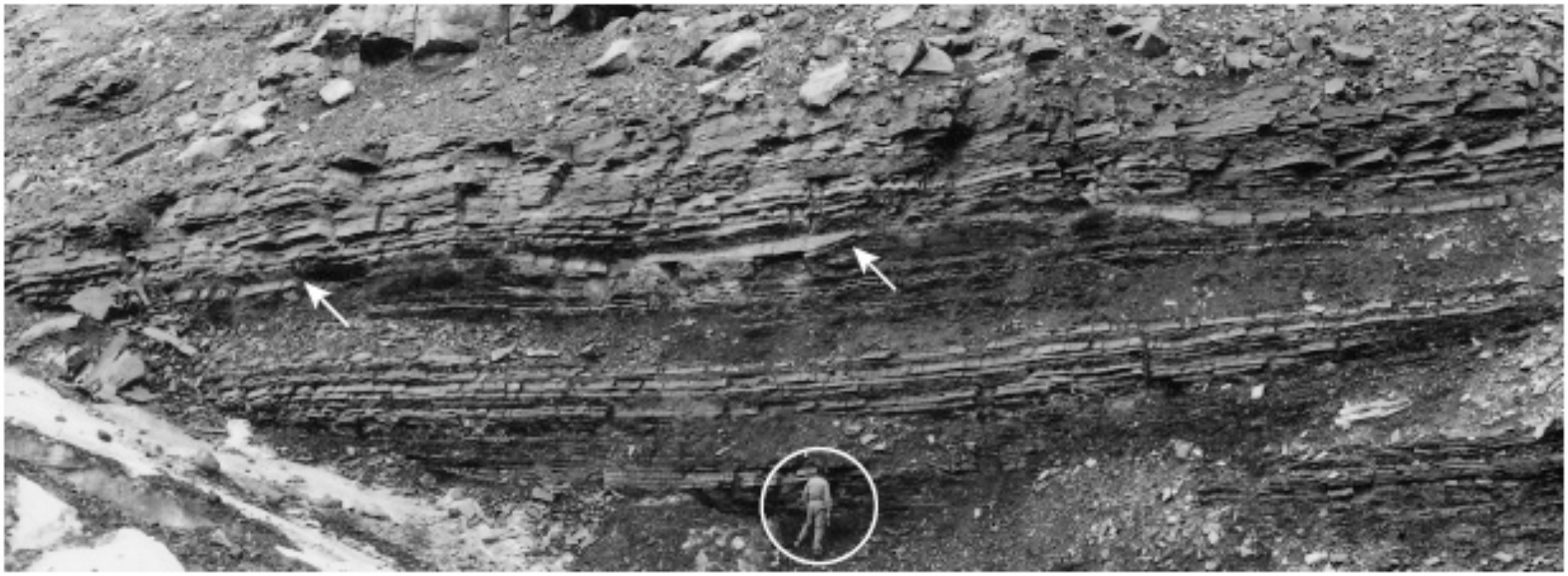

Figure 11—Outcrop photograph of the mudstone dominated levee of the lower Paleocene channel–levee succession (Figure 2, location 8). Note the laterally persistent thin-bedded turbidites. Minor sandstone-filled crevasse channels are marked by arrows. Person (circled) for scale.

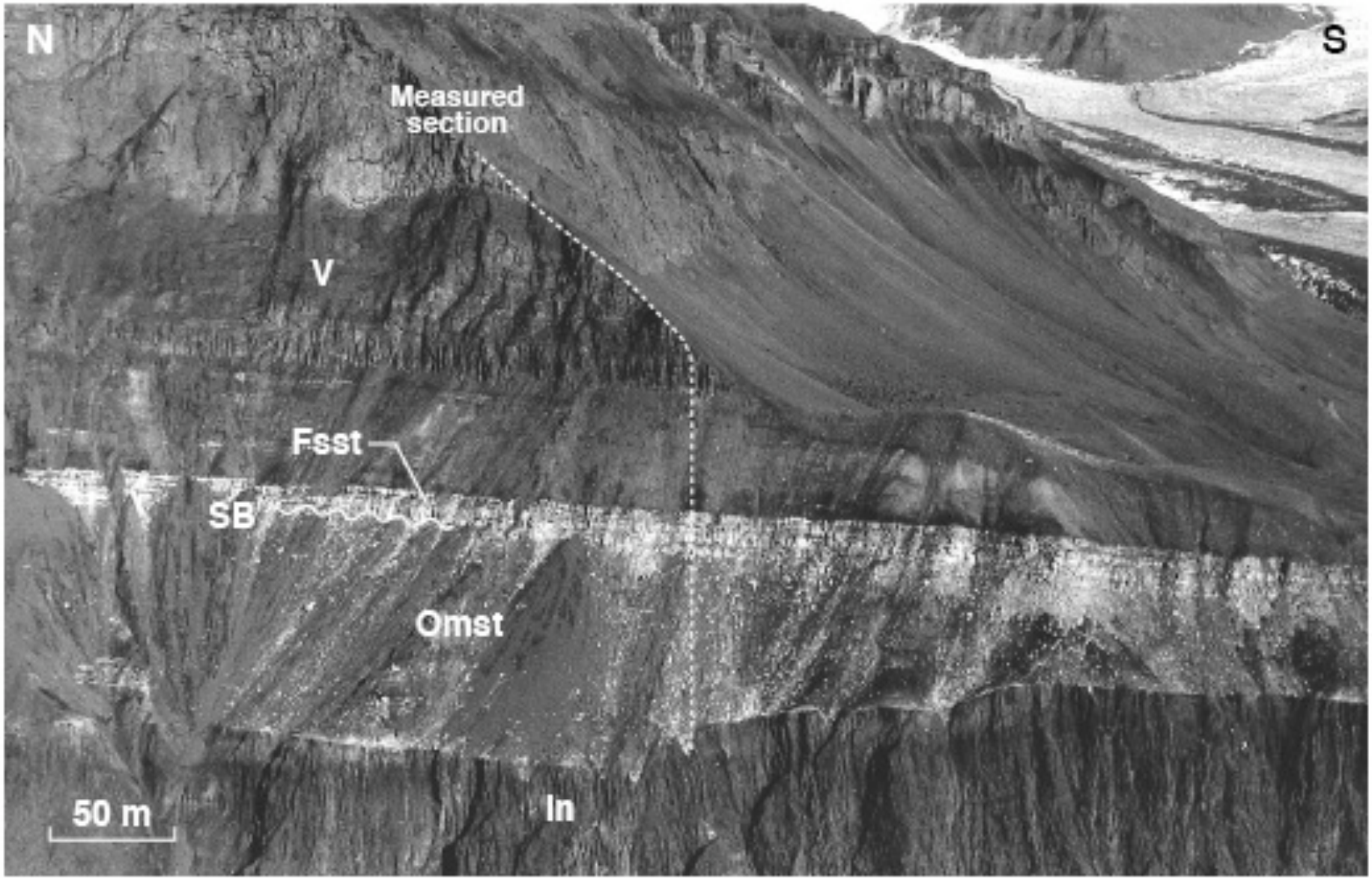

Figure 12—Mid-Paleocene pebbly fluvial sheet sandstone (Fsst) unconformably overlying offshore marine mudstones (Omst) north of Nansen Fjord (Figure 2, location 9). The unconformity is interpreted as representing a major sequence boundary (SB) forming the base of megasequence SQ2. The sandstone unit is up to 16 m thick and is overlain by a mudstone-dominated fluvial-plain succession grading upward into resedimented volcaniclastics (V) and lavas. In = Paleogene intrusive complex.

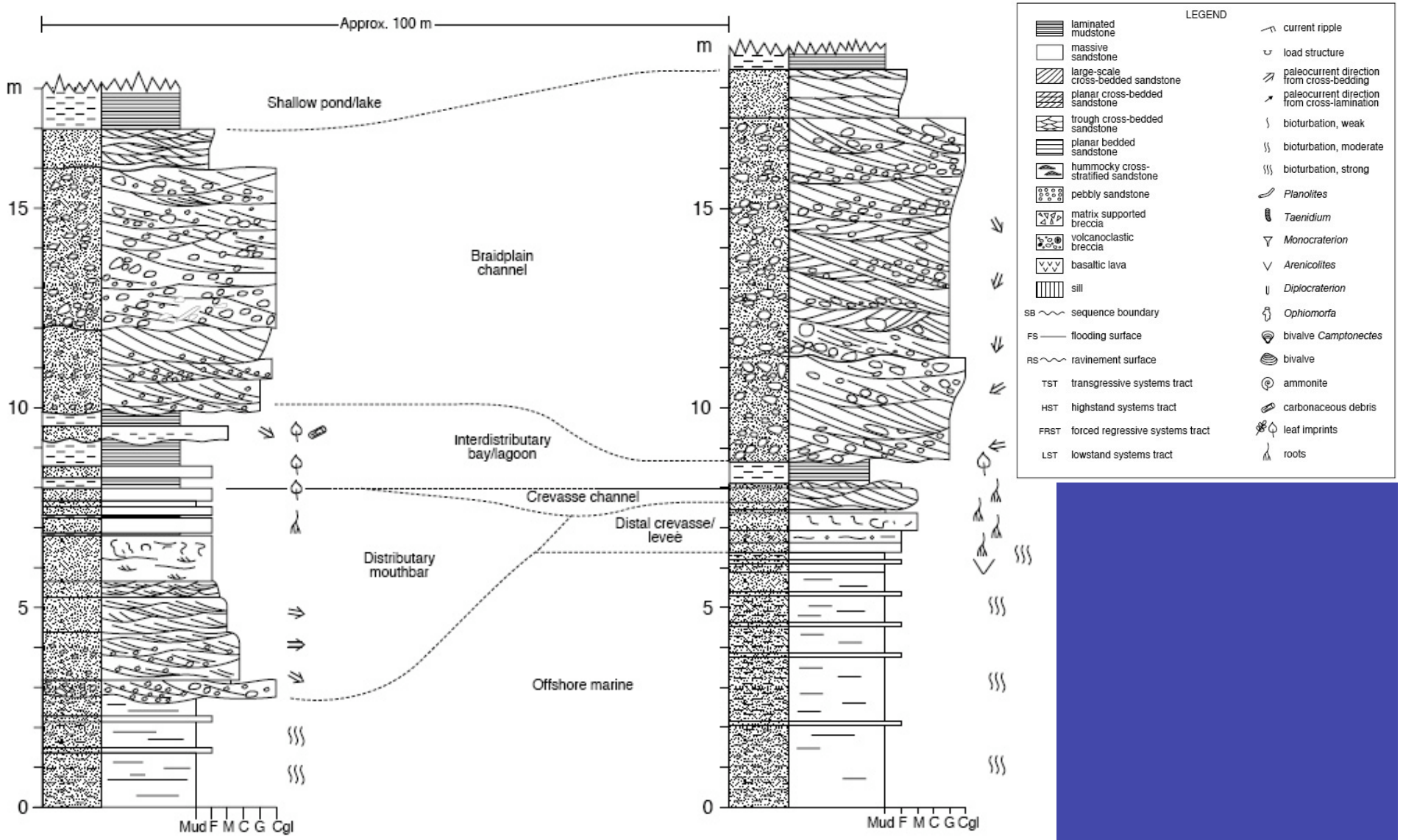

Figure 13—Vertical sections of the mid-Paleocene fluvial succession east of Sorgenfri Gletscher (Figure 2, location 8) showing the lateral variation of channel elements. The detailed sections correspond to the 165–184 m level in Figure 8. See Figure 6 for the legend.

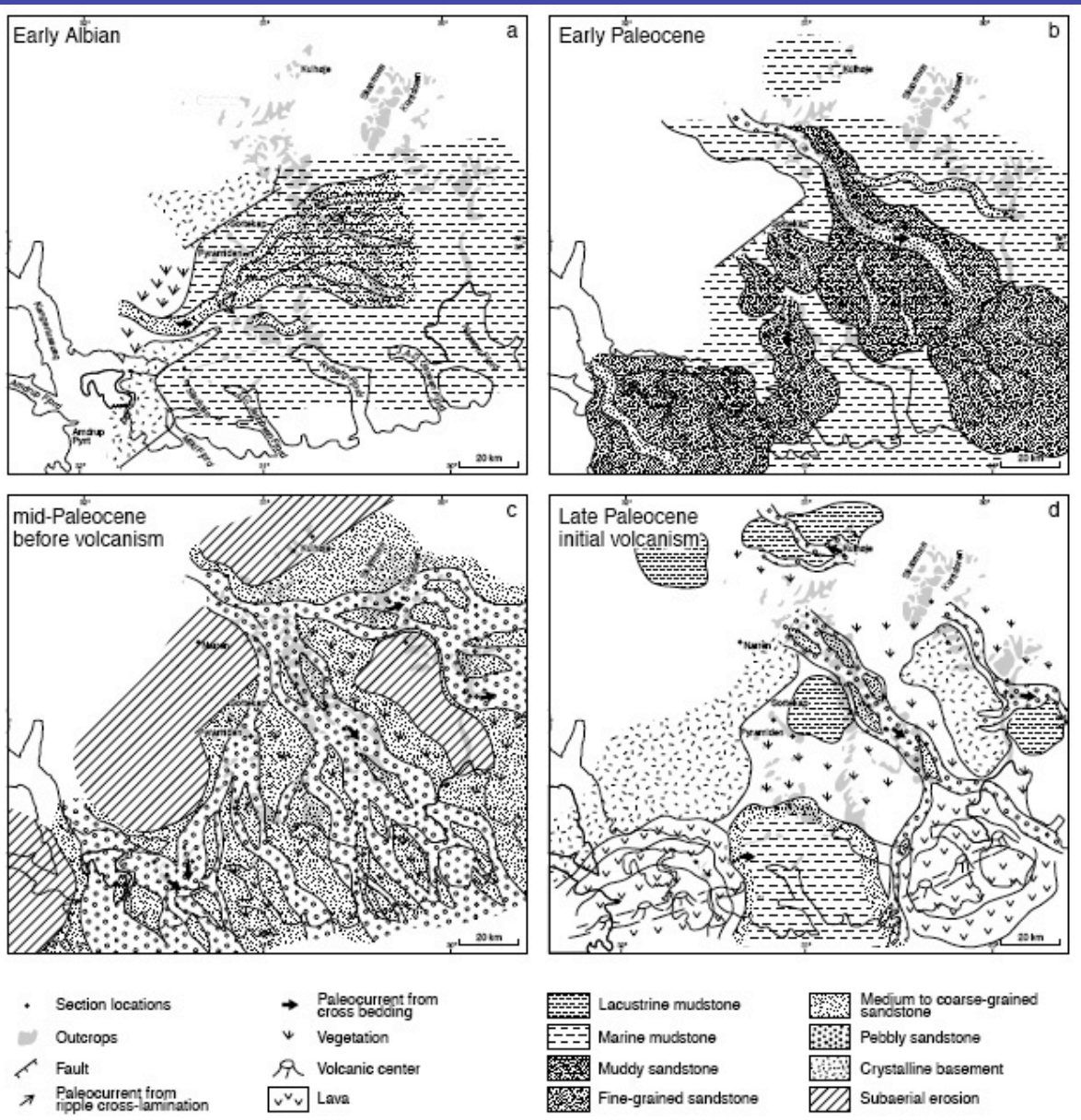

Figure 15—Paleogeography of the Kangerlussuaq basin during the Cretaceous–late Paleocene. (a) Early Albian axial fluvial drainage and estuary formed during an overall sea level rise following Aptian extension and basin formation. (b) Early Paleocene submarine fans prograding from the northwest during sea level highstand and early fall. (c) Mid-Paleocene (prevolcanic) regional uplift and erosion associated with sediment bypass and deposition of proximal braid-plain facies. (d) Late Paleocene initial volcanism associated with compartmentalization and local subsidence giving rise to pronounced lateral facies and thickness variations.

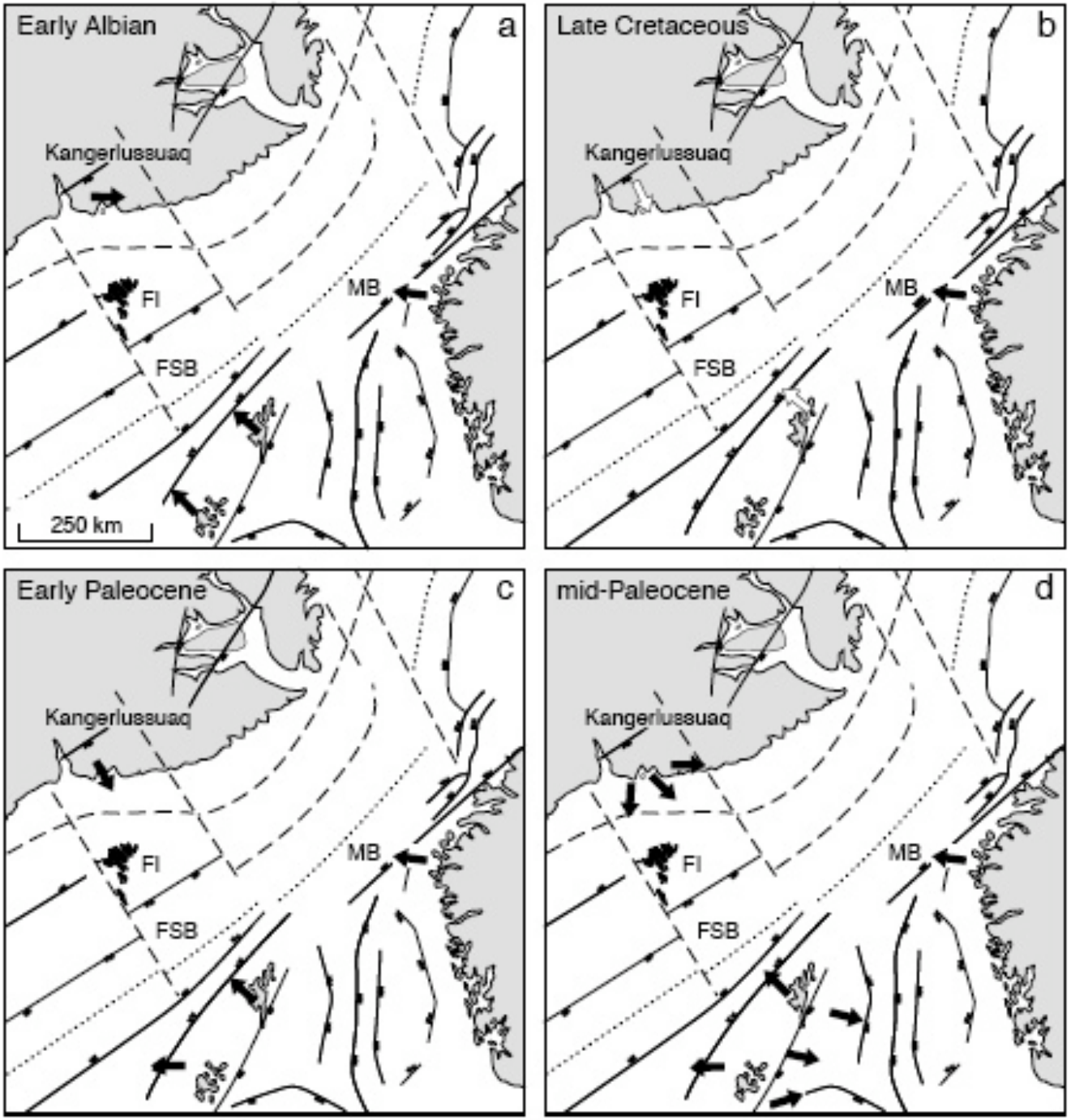

Figure 16—Summary of paleocurrent data from the Kangerlussuaq basin showing sediment transport directions relative to the suggested predrift position of the Faeroe Islands. Sand-prone sediments were supplied mainly during the (a) mid-Cretaceous (Aptian–Albian) and (b–d) latest Cretaceous–Paleocene. Substantial mid-Paleocen uplift of the North Atlant margins resulted in shedding of large volume of sediment into the sedimentary basins. Data for the Faeroe Basin are simplified from Knott et (1993). Black arrows = coarse-grained sediment, open arrows = mainly fine-grained sediment.

Conclusions

- Mid-Cretaceous alluvial plain, shallow marine, fluvio-esturine, and offshore marine sediments and early Paleocene submarine sediments
- Mid-Paleocene uplift
- Mid-Paleocene fluvial and deep burial by late Paleocene flood basalts
- Middle Eocene-early?Oligocene uplift associated with North Atlantic rifting and seafloor spreading

Subsidence of the Atlantic-type Continental Margin off New York

Steckler and Watts 1978

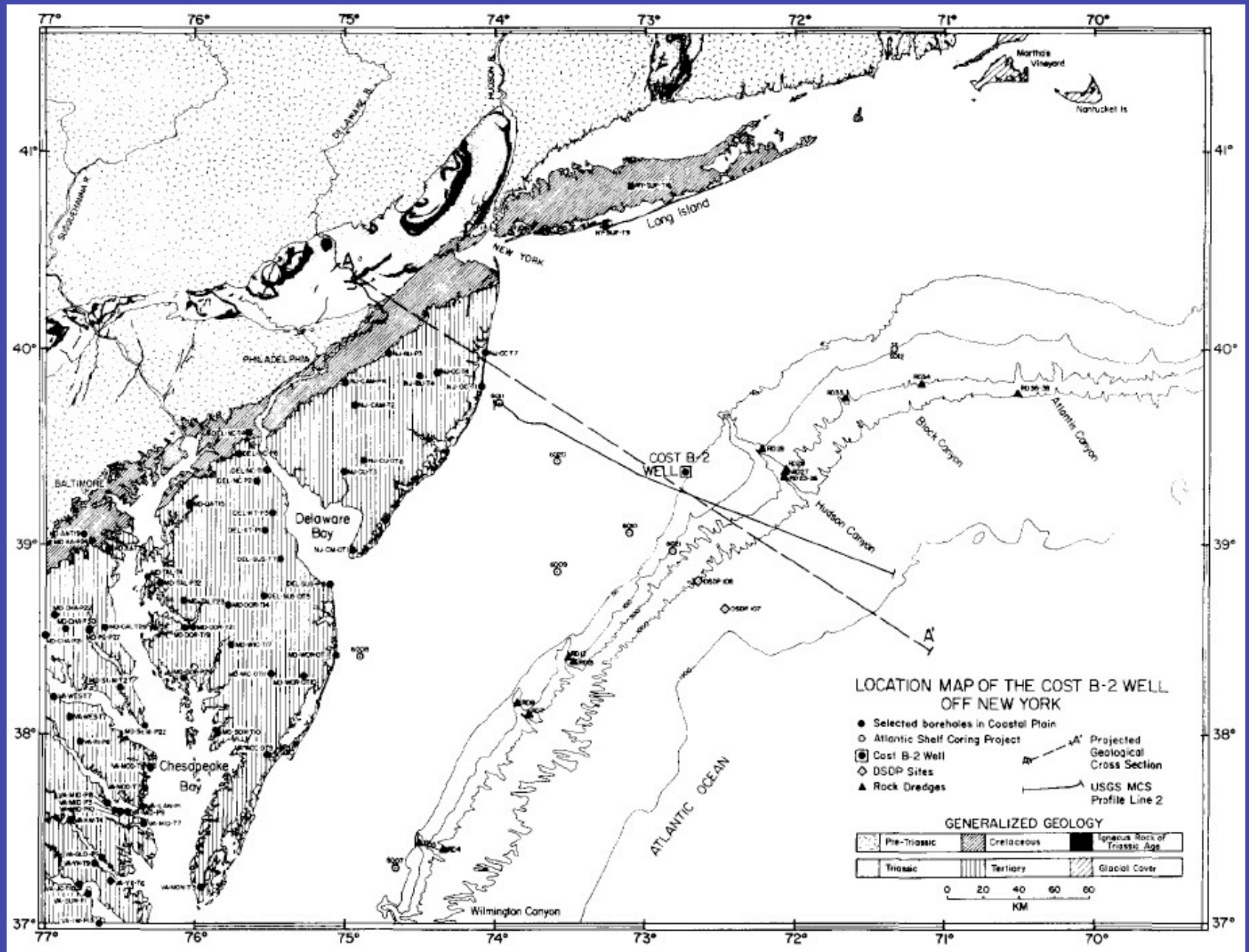

Fig. 1. Location map of the COST B-2 well [6] on the outer continental shelf off New York. The location of other boreholes is based on Brown et al. [33] for the coastal plain and Hathaway et al. [34] for the Atlantic shelf and slope. The location and identification of the rock dredges are from a compilation by Gibson et al. [35].

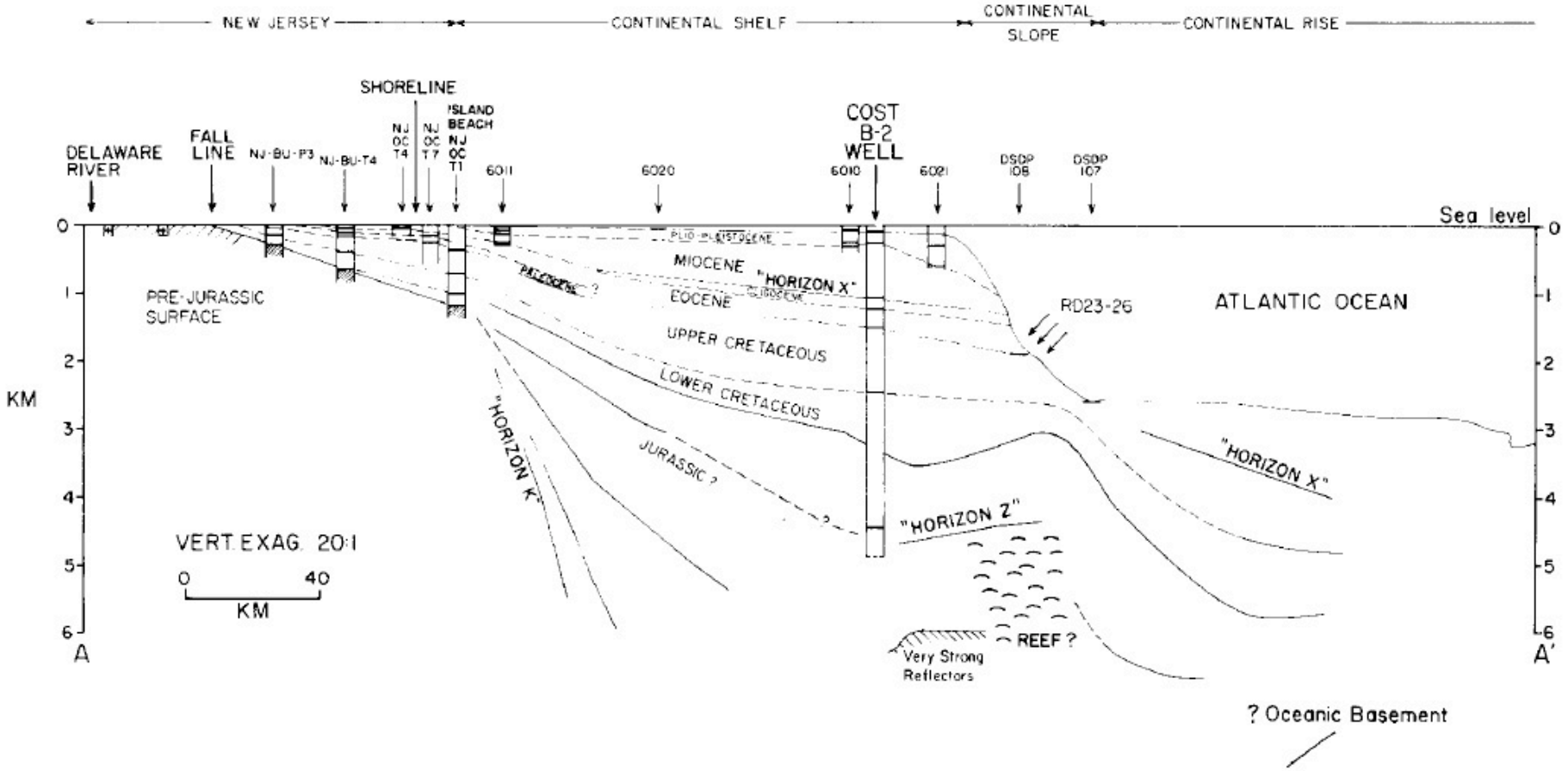

Fig. 2. Schematic cross-section of the continental shelf and margin off New York along profile A-A' (Fig. 1). The identification of sedimentary horizons is based mainly on the COST B-2 well and other boreholes in the shelf and margin. The continuity of sedimentary horizons between boreholes is based on the nearby multichannel Line 2 ([4]; Fig. 1). The solid lines in the cross-section are based on prominent seismic horizons summarized in fig. 11 of Schlee et al. [4].

Well COST B-2 has over 4000 meters of shallow water sediments. Airy isostacy indicates that 1000 meters of sedimentation should yield 600 meters of subsidence. What else is going on here?

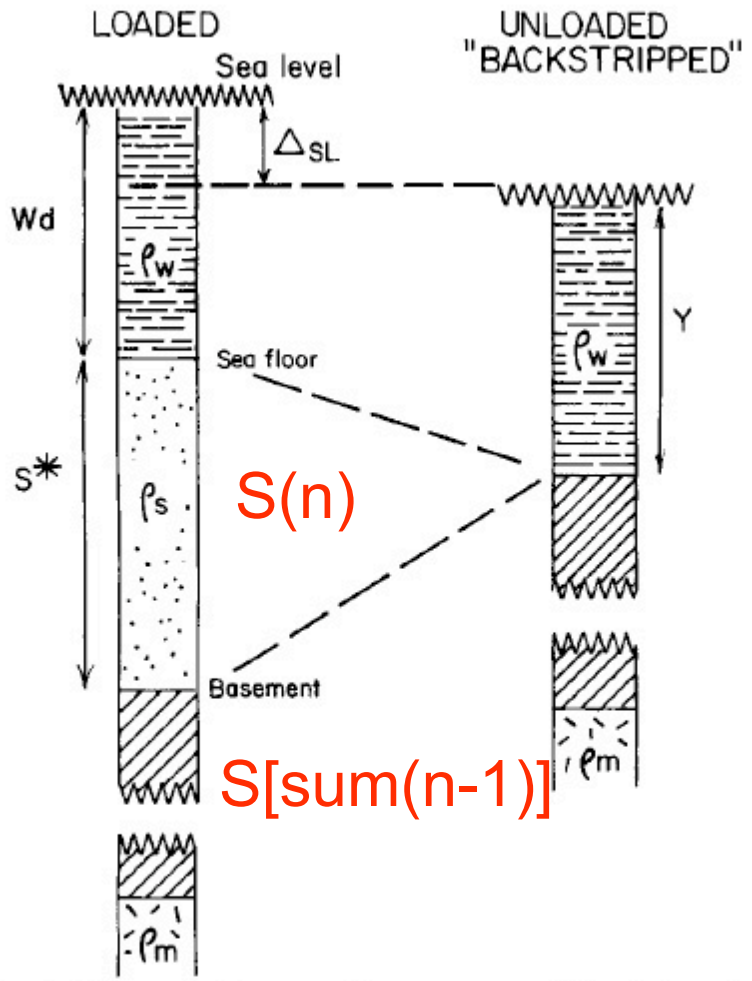

Fig. 3. Schematic diagram of a reconstructed (loaded) sedimentary section and a "backstripped" (unloaded) sedimentary section. The parameters are defined in the text.

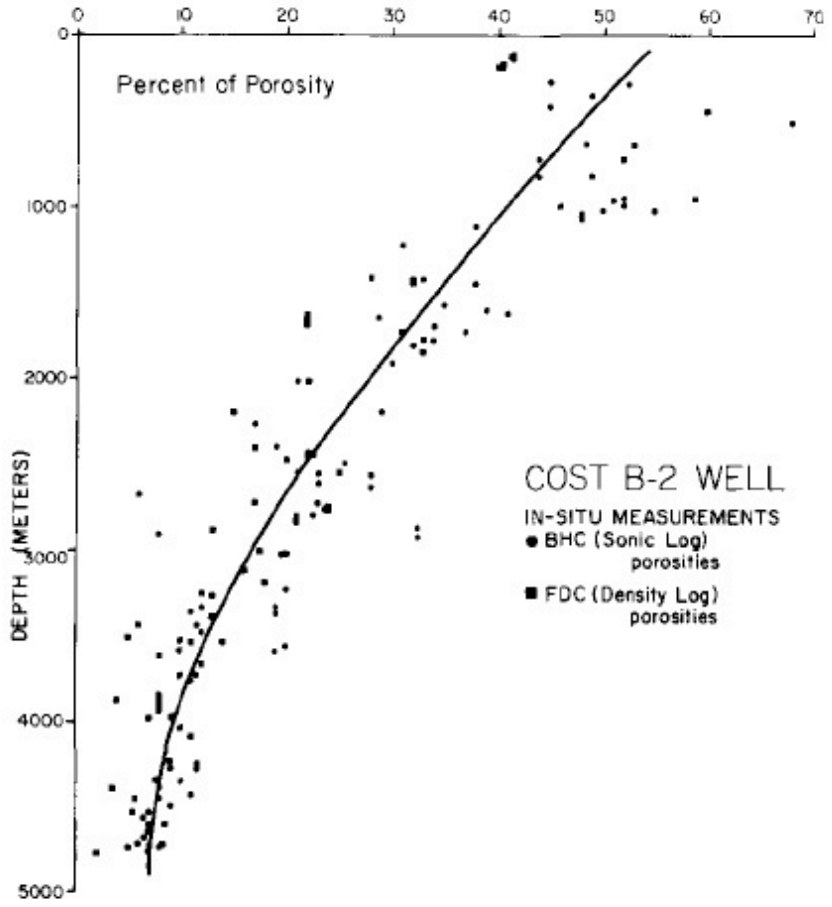

Fig. 4. Porosity-depth curve for the COST B-2 well based on data tabulated by Rhodehamel [21]. The heavy line indicates a "smooth" curve assumed in the computation of the reconstructed sedimentary section.

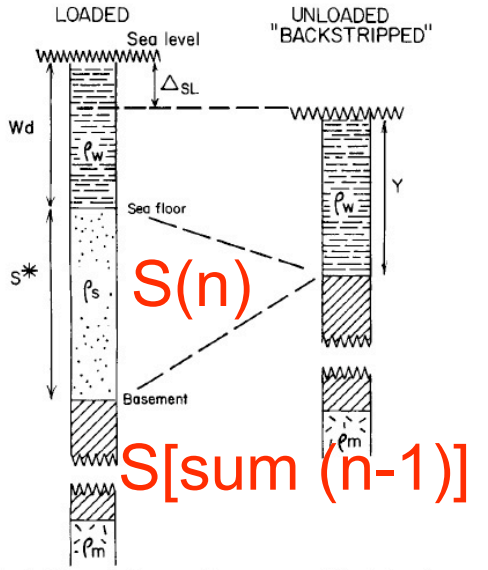

Fig. 3. Schematic diagram of a reconstructed (loaded) sedimentary section and a "backstripped" (unloaded) sedimentary section. The parameters are defined in the text.

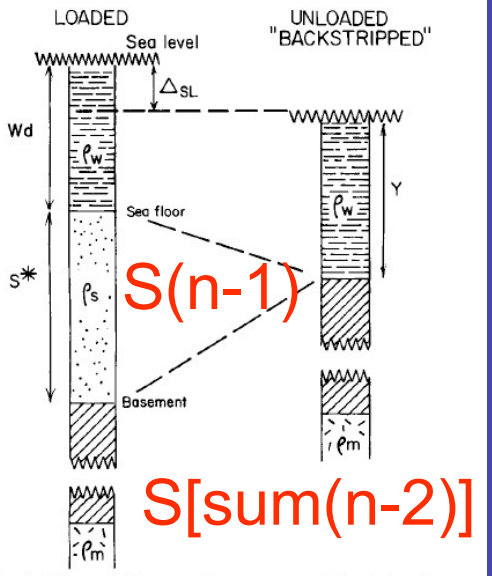

Fig. 3. Schematic diagram of a reconstructed (loaded) sedimentary section and a "backstripped" (unloaded) sedimentary section. The parameters are defined in the text.

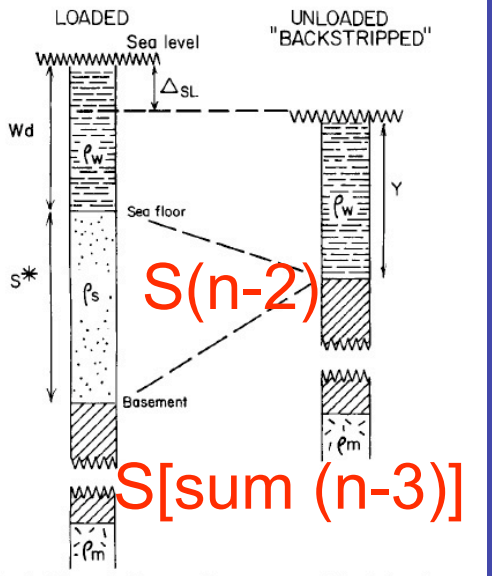

Fig. 3. Schematic diagram of a reconstructed (loaded) sedimentary section and a "backstripped" (unloaded) sedimentary section. The parameters are defined in the text.

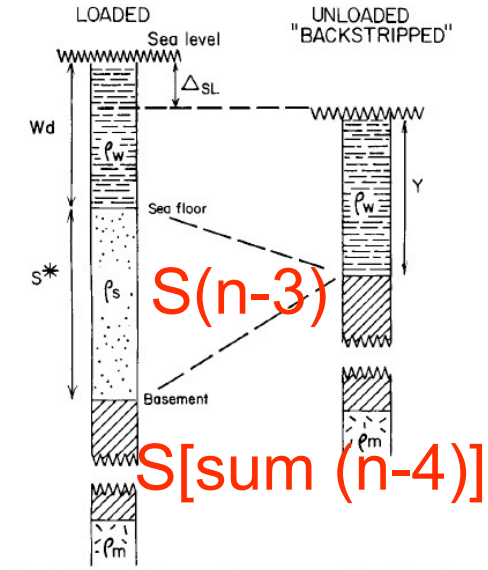

Fig. 3. Schematic diagram of a reconstructed (loaded) sedimentary section and a "backstripped" (unloaded) sedimentary section. The parameters are defined in the text.

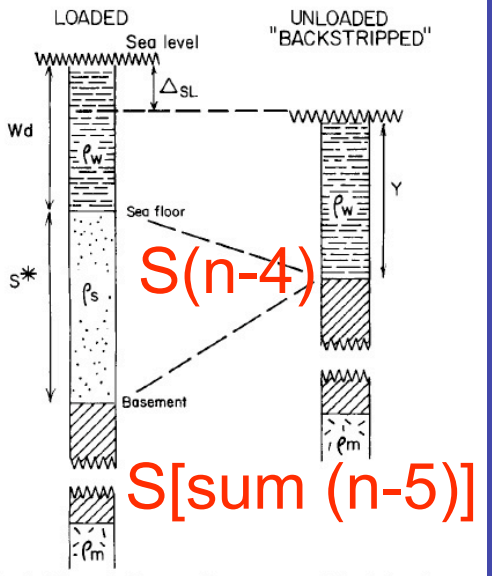

Fig. 3. Schematic diagram of a reconstructed (loaded) sedimentary section and a "backstripped" (unloaded) sedimentary section. The parameters are defined in the text.

Etc

TABLE 1

Summary of total sediment thicknesses, porosity, water depth and sea-level change through time for the COST B-2 well off New York

	Age (m.y. B.P.)	Horizon depth (ft)	Total sediment thickness (ft)	Porosity (%)	Corrected sediment thickness (ft)	Water depth (ft)	Sea-level change (ft)	Sea-level correction (ft)	Computed basement depth					
									local loading (ft)		flexural loading			
											present-day shelf (ft)		eroded shelf (ft)	
Plio-Pleistocene	0	0	42,000	54.0	42,000	0–90	302	433	16,866	16,956	20,047	20,137		
U. Miocene	5	522	41,478	52.5	41,734	0–50	302	433	16,769	16,819	19,895	19,945		
M. Miocene	11.4	784	41,216	46.0	41,597	0–300	272	390	16,762	17,062	19,848	20,148	same as present-day shelf	
L. Miocene	15.7	3169	38,831	41.0	40,148	3–600	272	390	16,547	16,847	19,413	19,713		
U. Oligocene	22.5	3208	38,792	39.5	40,159	3–600	374	522	16,406	16,706	19,249	19,549		
L. Oligocene	32.5	3623	38,377	38.5	39,885	3–600	496	715	16,113	16,413	18,883	19,183		
U. Eocene	38	3694	38,306	38.0	39,837	3–600	618	889	15,922	16,222	18,669	18,969	17,921	18,221
M. Eocene	44	3816	38,184	37.5	39,755	3–1500	692	993	15,788	16,988	18,535	19,735	17,777	18,977
L. Eocene	49	4241	37,759	36.5	39,465	3–1500	804	1153	15,522	16,722	18,239	19,439	17,480	18,680
Paleocene	55	4576	37,424	35.5	39,233	3–1500	866	1242	15,349	16,549	18,044	19,244	17,278	18,478
Maastrichtian	65	4612	37,388	35.0	39,208	3–1500	1089	1562	15,020	16,220	17,733	18,933	16,949	18,149
Campanian	72.5	4712	37,288	34.0	39,137	3–1500	1144	1642	14,914	16,114	17,662	18,862	16,876	18,076
Santonian	80	5348	36,652	32.0	38,680	3–1500	1144	1642	14,748	15,948	17,473	18,673	16,693	17,893
Sant.-Con.	83	5675	36,325	29.5	38.438	0–50	1133	1628	14,373	14,423	17,050	17,100	16,276	16,326
Turonian	88	6609	35,391	26.0	37,678	3–600	1059	1534	14,490	14,790	17,112	17,412	16,354	16,654
Cenomanian	94	7222	34,778	24.0	37,235	3–600	988	1402	14,461	14,761	17,049	17,349	16,310	16,610
Albian	100	7742	34,258	22.0	36,807	0–600	833	1195	14,212	14,812	16,771	17,371	16,023	16,623
Aptian	106	8512	33,488	19.0	36,158	0–300	642	922	14,249	14,549	16,762	17,062	15,997	16,297
Barremian	112	9612	32,388	16.0	35,196	0–300	491	706	14,114	14,414	16,528	16,828	15,755	16,055
Haut.-Val.	118	10,612	31,388	13.0	34,290	0–300	409	588	13,902	14,202	16,210	16,510	15,445	15,745
Berriasian	130	11,612	30,388	10.0	33,353	0–50	376	541	13,608	13,658	15,879	15,929	15,063	15,113
Jurassic (?)	135	14,262	27,738	7.5	30,786	0–50	376	541	12,673	12,723	14,575	14,625	13,806	13,856
Base of B-2	134–141	15,655	26,345	7.0	29,400	0–50	219–376	325–541	12,168	12,326	13,892	14,050	13,243	13,401
Basement	195 (?)	42,000	0	–	0	0	0–75	0–108	0	108	0	108	0	108

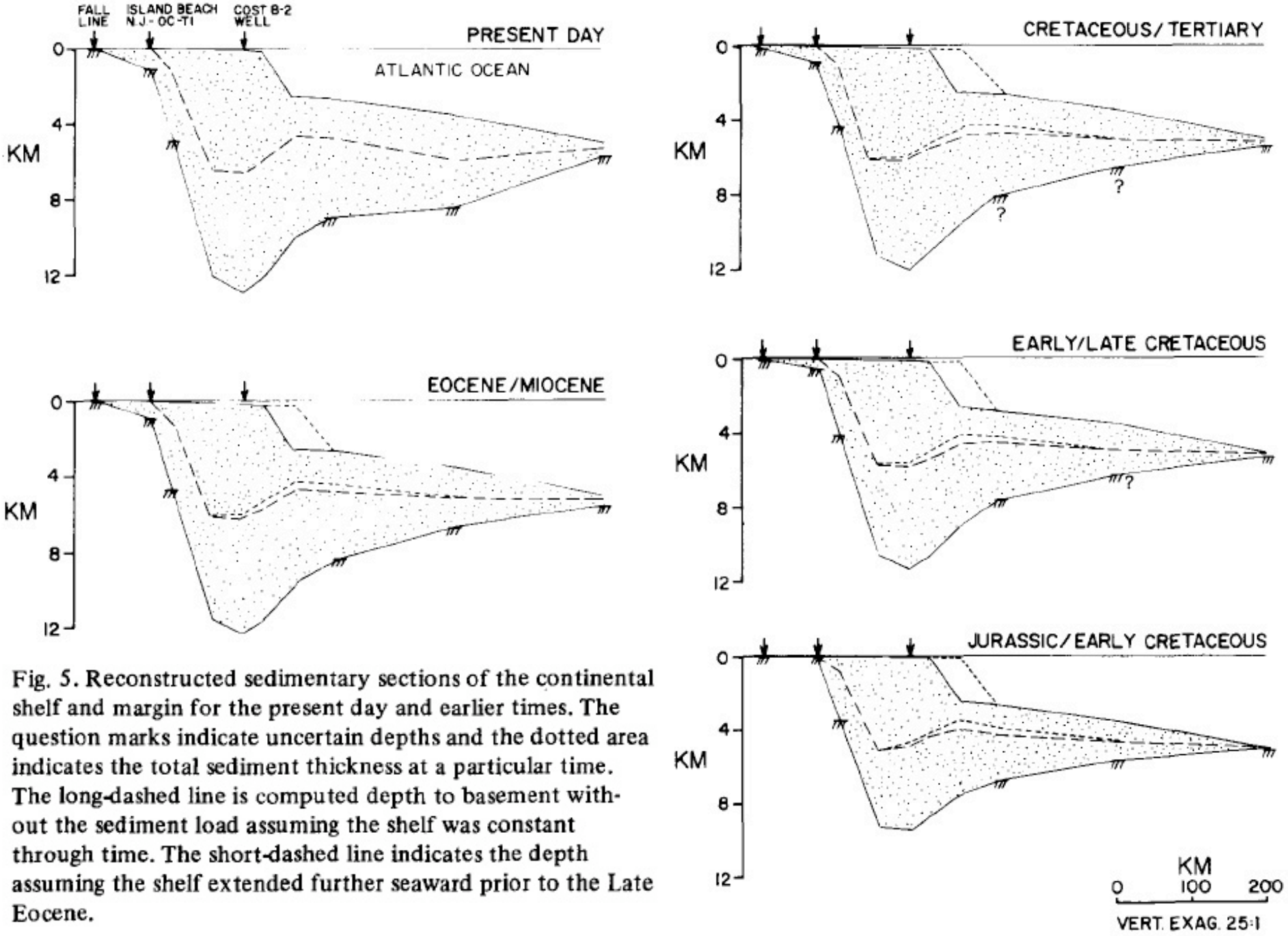

Fig. 5. Reconstructed sedimentary sections of the continental shelf and margin for the present day and earlier times. The question marks indicate uncertain depths and the dotted area indicates the total sediment thickness at a particular time. The long-dashed line is computed depth to basement without the sediment load assuming the shelf was constant through time. The short-dashed line indicates the depth assuming the shelf extended further seaward prior to the Late Eocene.

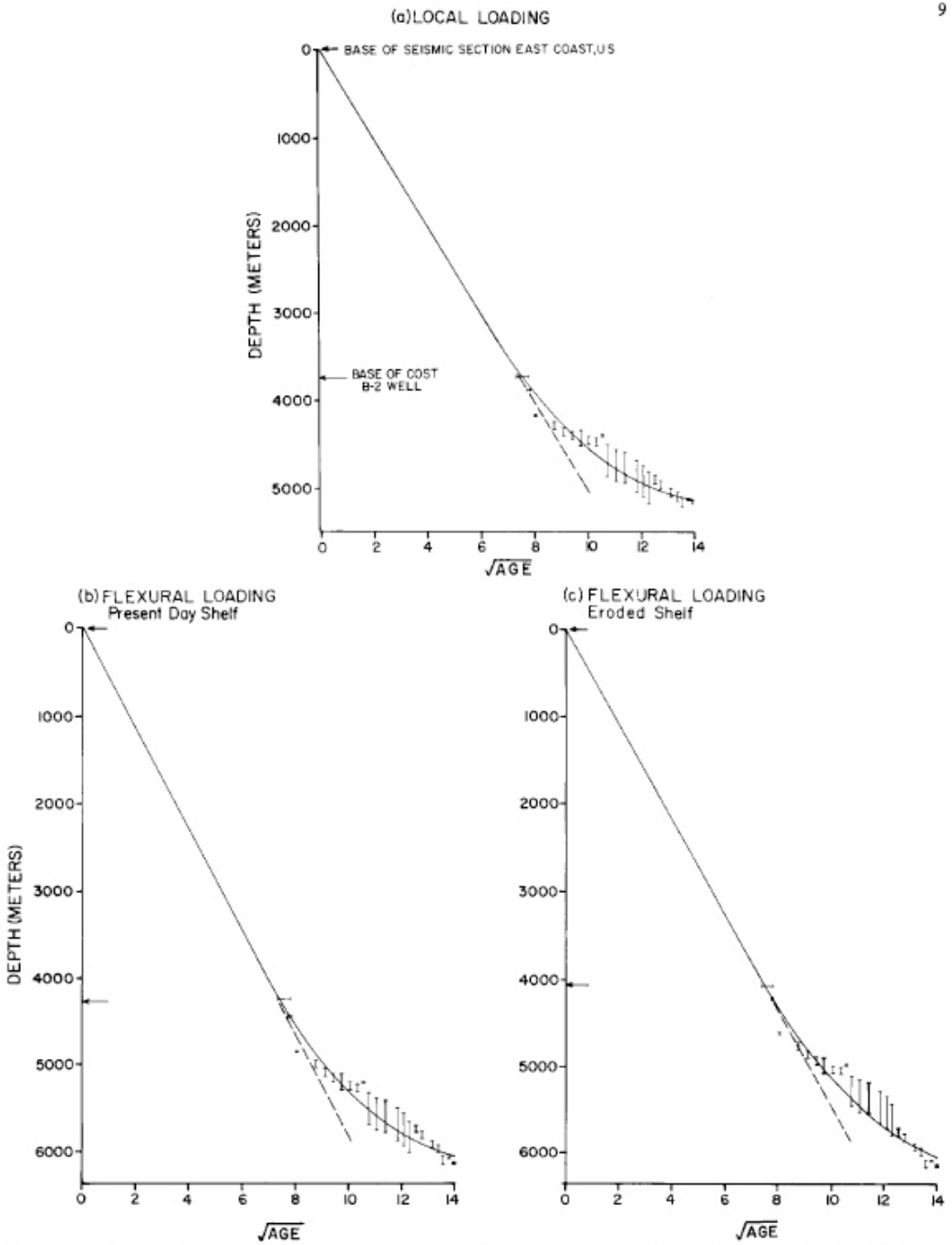

Fig. 7. Plot of depth against $(age)^{1/2}$ for three models of "backstripping" sediments from the margin. The age assumed for the start of the subsidence is 195 m.y. B.P. [27]. The vertical bars reflect the range of water depth.

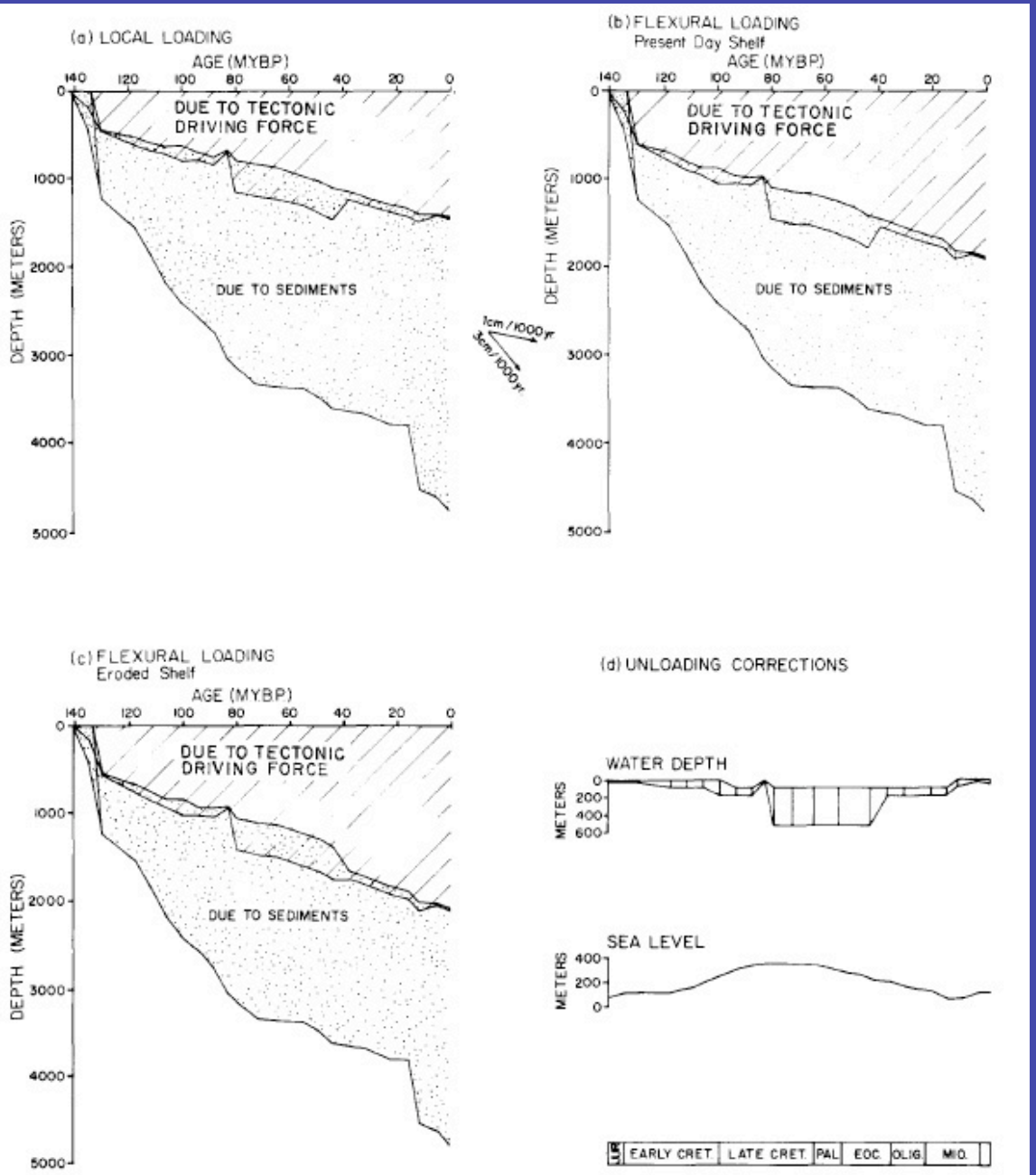

Fig. 6. Summary of subsidence curves for the COST B-2 well for three models of "backstripping" sediments from the margin. In each model the dotted area indicates that part of the observed subsidence which can be attributed to sediment loading and the cross-hatched area indicates that part which can be attributed to other "tectonic driving forces". Fig. 6d is a plot of the water depth and sea-level corrections used to "backstrip" the sediments from the margin.

Conclusions

- 4.8 km of shallow water sediments at Cost 2B well are not due to sediment loading of the crust alone
- “Tectonic driving forces” contribute to crust subsidence at Cost 2B
- Parsons and Sclater thermal model almost accounts for subsidence
- Crustal thinning plays a role in subsidence at Cost 2B.